Published OnlineFirst April 18, 2012; DOI:10.1158/1078-0432.CCR-12-0183

and they require defense against ROS to survive (31). Many studies have already reported that GPX1 may protect cancer cells under conditions of severe oxidative stress as it has been observed that increased GPX1 activity can inhibit apoptosis (14, 15), reduce tumor sensitivity toward ROS-generating anticancer drugs (17, 18), and promote the more malignant stages of cancer (16). Our findings showed that SBP1 could greatly inhibit the activity, but not expression, of GPX1 in cancer cells both *in vitro* and *in vivo*; the translocation of GPX1 to the nucleus in cancer cells under oxidative stress may facilitate the antioxidant functions of GPX1, whereas the formation and combination of GPX1 and SBP1 nuclear bodies might inhibit this process. The formation of this SBP1-GPX1 complex has also been validated by coimmunoprecipitation in a prior study, which suggested that this phenomenon was a direct physical interaction (19). We also noticed the expression level of SBP1 was upregulated by oxidative stress (Fig. 2C). Normally, the high level of oxidative stress in cancer cells (usually caused by tumor microenvironment or drug-induced ROS) would lead to cellular apoptosis rather than survival or transformation due to the inhibition of GPX1 activity by the upregulated SBP1. However, as the expression of SBP1 in HCC and many other cancers was reduced (mechanisms might include DNA methylation and chromatin remodeling; ref. 32), the intensive oxidative stress in the tumor microenvironment could be attenuated by the activation of GPX1, leading to cancer cell survival, proliferation, malignant transformation, and even metastasis (31).

We observed a relationship among SBP1, HIF-1α, and ROS. ROS could initiate the activation of HIF-1α (21), whereas HIF-1α could regulate the expression of SBP1 through a hypoxia response element in its promoter region (20). On the basis of this effect, ROS would elevate the expression of SBP1 through HIF-1α mediation. This was supported by our Western blotting results as showed in Fig. 2C. However, we further observed that the SBP1-silenced cancer cells had a diminished HIF-1α expression under oxidative stress, which indicated that SBP1 could somehow counter-regulate the expression of HIF-1α during cellular oxidative stress (Fig. 2C). A possible explanation for this phenomenon was that the exogenous ROS in SBP1-silenced cells was immediately degraded by GPX1, leading to diminished HIF-1α expression. It has been reported that HIF-1α can suppress the epithelial–mesenchymal transition through the p53 pathway (also, ROS is a well-known initiator of p53-mediated apoptosis; ref. 33) and inhibit malignant tumor conversion (20, 34, 35). This might also be the reason for the increased malignancy and invasive characteristics of tumors with low SBP1 expression. We illustrated the possible relationship of SBP1, GPX1, HIF-1α, and ROS (Fig. 5C).

As most of the anticancer agents kill tumor cells by generating ROS or amplifying oxidative stress (31, 36, 37), we concluded that increased SBP1 expression and decreased GPX1 activity could elevate tumor chemosensitivity. This conclusion was supported by several previous studies, which investigated SBP1 and GPX1 separately (8, 18, 38). On the other hand, the poor responses of patients with HCC to chemotherapy might be due to low SBP1 expression and high GPX1 activity, thus increasing SBP1 expression and decreasing GPX1 activity could be a novel strategy for cancer treatment. However, SBP1 and GPX1 are both selenium-containing proteins, and attempts to reduce cancer risk by simple selenium supplementation in the Selenium and Vitamin E Cancer Prevention Trial (SELECT) have already failed (39). However, recent studies have found certain forms of selenium (such as SeL) can act as pro-oxidants rather than antioxidants and have chemotherapeutic potential by inducing cancer cell apoptosis while leaving normal cells unaffected (40, 41). These certain forms of selenium might exclusively elevate the level of SBP1 rather than GPX1, which might provide a new tool in cancer treatment but requires further investigation.

Our clinical data validated the possible role of SBP1 in cancer biology. Patients with positive SBP1 expression experienced longer periods of OS and lower recurrence rates, indicating that negative SBP1 expression could be a potential biomarker predicting early recurrence/poor prognosis and guide our follow-up treatment in patients with HCC after surgery. When we further stratified patients by Milan criteria, which are widely accepted guidelines for early stage liver transplantation, the survival curves in this study show that negative SBP1 expression in the tumor cells correlated with higher early recurrence rates in patients within the Milan criteria. However, no significant difference was observed with regard to survival periods, thus the predictive significance of SBP1 in this subpopulation would help clinicians identify patients at high risk of early recurrence and enable them to administer rational adjuvant therapy after resection or liver transplantation. However, we noticed that SBP1 is a more effective predictor for patients with HCC beyond the Milan criteria rather than for those within the Milan criteria (Fig. 6C and D). This could be understood by the role of SBP1 in the tumor redox microenvironment considering that patients in the advanced stages of cancer often suffer from more severe hypoxia and oxidative stress than those in the early stages. On the basis of this conclusion, treatment of patients beyond the Milan criteria with SBP1 positive expression should be more aggressive, for these patients can also achieve excellent survival outcomes. Furthermore, the use of glutathione treatment in patients with cancer, especially advanced-stage cancers, should be completed with caution, for glutathione may elevate the activity of GPX1 and promote tumor development based on our findings and those of other groups (42). Taken together, our data indicate that SBP1 is a tumor biomarker with prognostic value in patients with HCC. Determination of SBP1 expression may be useful for personalized therapeutic strategies and decisions about individuals outside of the Milan criteria who could benefit from more aggressive treatment, such as liver transplantation. Currently, the outcomes of these patients are very difficult to predict using conventional clinical indices.

In conclusion, decreased expression of SBP1 could lead to higher GPX1 activity and a diminished HIF-1α expression in

Published OnlineFirst April 18, 2012; DOI:10.1158/1078-0432.CCR-12-0183

HCC; thus, SBP1 might exert its tumor suppressive function as a regulator of the tumor redox microenvironment. SBP1 could be a novel biomarker for predicting prognosis and guiding personalized therapeutic strategies, especially in patients with advanced HCC.

Disclosure of Potential Conflicts of Interest

No potential conflicts of interest were disclosed.

Authors' Contributions

Conception and design: C. Huang, G. Ding, C. Gu, T. Kondo, J. Fan
Development of methodology: C. Huang, G. Ding, Y. Ji, T. Kondo
Acquisition of data (provided animals, acquired and managed patients, provided facilities, etc.): C. Huang, C. Gu, J. Zhou, Y. He, T. Kondo, J. Fan
Analysis and interpretation of data (e.g., statistical analysis, biostatistics, computational analysis): C. Huang, G. Ding, C. Gu, J. Zhou, M. Kuang, Y. Ji, Y. He, T. Kondo, J. Fan
Writing, review, and/or revision of the manuscript: C. Huang, G. Ding, C. Gu, J. Zhou, M. Kuang, T. Kondo, J. Fan
Administrative, technical, or material support (i.e., reporting or organizing data, constructing databases): C. Huang, C. Gu, J. Zhou, T. Kondo, J. Fan
Study supervision: C. Huang, C. Gu, T. Kondo, J. Fan

Grant Support

The study was supported by grants from the National Natural Science Foundation of China (NSFC; no. 30600605), the Major Program of NSFC (no. 81030038), and the National Key Sci-Tech Project of China (2008ZX10002-019).

The costs of publication of this article were defrayed in part by the payment of page charges. This article must therefore be hereby marked *advertisement* in accordance with 18 U.S.C. Section 1734 solely to indicate this fact.

Received January 20, 2012; revised March 2, 2012; accepted March 18, 2012; published OnlineFirst April 18, 2012.

References

1. Rayman MP. The importance of selenium to human health. Lancet 2000;356:233–41.
2. Chang PW, Tsui SK, Liew C, Lee CC, Waye MM, Fung KP. Isolation, characterization, and chromosomal mapping of a novel cDNA clone encoding human selenium binding protein. J Cell Biochem 1997;64:217–24.
3. Whanger PD. Selenium and its relationship to cancer: an update. Br J Nutr 2004;91:11–28.
4. Papp LV, Holmgren A, Khanna KK. Selenium and selenoproteins in health and disease. Antioxid Redox Signal 2010;12:793–5.
5. Kryukov GV, Gladyshev VN. Mammalian selenoprotein gene signature: identification and functional analysis of selenoprotein genes using bioinformatics methods. Methods Enzymol 2002;347:84–100.
6. Brigelius-Flohe R. Selenium compounds and selenoproteins in cancer. Chem Biodivers 2008;5:389–95.
7. Li T, Yang W, Li M, Byun DS, Tong C, Nasser S, et al. Expression of selenium-binding protein 1 characterizes intestinal cell maturation and predicts survival for patients with colorectal cancer. Mol Nutr Food Res 2008;52:1289–99.
8. Silvers AL, Lin L, Bass AJ, Chen G, Wang Z, Thomas DG, et al. Decreased selenium-binding protein 1 in esophageal adenocarcinoma results from posttranscriptional and epigenetic regulation and affects chemosensitivity. Clin Cancer Res 2010;16:2009–21.
9. Kim H, Kang HJ, You KT, Kim SH, Lee KY, Kim TI, et al. Suppression of human selenium-binding protein 1 is a late event in colorectal carcinogenesis and is associated with poor survival. Proteomics 2006;6:3466–76.
10. Chen G, Wang H, Miller CT, Thomas DG, Gharib TG, Misek DE, et al. Reduced selenium-binding protein 1 expression is associated with poor outcome in lung adenocarcinomas. J Pathol 2004;202:321–9.
11. Huang KC, Park DC, Ng SK, Lee JY, Ni X, Ng WC, et al. Selenium binding protein 1 in ovarian cancer. Int J Cancer 2006;118:2433–40.
12. He QY, Cheung YH, Leung SY, Yuen ST, Chu KM, Chiu JF. Diverse proteomic alterations in gastric adenocarcinoma. Proteomics 2004;4:3276–87.
13. Corona G, De Lorenzo E, Elia C, Simula MP, Avellini C, Baccarani U, et al. Differential proteomic analysis of hepatocellular carcinoma. Int J Oncol 2010;36:93–9.
14. Faucher K, Rabinovitch-Chable H, Cook-Moreau J, Barriere G, Sturtz F, Rigaud M. Overexpression of human GPX1 modifies Bax to Bcl-2 apoptotic ratio in human endothelial cells. Mol Cell Biochem 2005;277:81–7.
15. de Haan JB, Bladier C, Griffiths P, Kelner M, O'Shea RD, Cheung NS, et al. Mice with a homozygous null mutation for the most abundant glutathione peroxidase, Gpx1, show increased susceptibility to the oxidative stress-inducing agents paraquat and hydrogen peroxide. J Biol Chem 1998;273:22528–36.
16. Ho JC, Chan-Yeung M, Ho SP, Mak JC, Ip MS, Ooi GC, et al. Disturbance of systemic antioxidant profile in nonsmall cell lung carcinoma. Eur Respir J 2007;29:273–8.
17. Lee WP, Lee CL, Lin HC. Glutathione S-transferase and glutathione peroxidase are essential in the early stage of adriamycin resistance before P-glycoprotein overexpression in HOB1 lymphoma cells. Cancer Chemother Pharmacol 1996;38:45–51.
18. Vibet S, Goupille C, Bougnoux P, Steghens JP, Gore J, Maheo K. Sensitization by docosahexaenoic acid (DHA) of breast cancer cells to anthracyclines through loss of glutathione peroxidase (GPx1) response. Free Radic Biol Med 2008;44:1483–91.
19. Fang W, Goldberg ML, Pohl NM, Bi X, Tong C, Xiong B, et al. Functional and physical interaction between the selenium-binding protein 1 (SBP1) and the glutathione peroxidase 1 selenoprotein. Carcinogenesis 2010;31:1360–6.
20. Scortegagna M, Martin RJ, Kladney RD, Neumann RG, Arbeit JM. Hypoxia-inducible factor-1alpha suppresses squamous carcinogenic progression and epithelial-mesenchymal transition. Cancer Res 2009;69:2638–46.
21. Pouyssegur J, Mechta-Grigoriou F. Redox regulation of the hypoxia-inducible factor. Biol Chem 2006;387:1337–46.
22. Parkin DM, Bray F, Ferlay J, Pisani P. Global cancer statistics, 2002. CA Cancer J Clin 2005;55:74–108.
23. Thomas MB, O'Beirne JP, Furuse J, Chan AT, Abou-Alfa G, Johnson P. Systemic therapy for hepatocellular carcinoma: cytotoxic chemotherapy, targeted therapy and immunotherapy. Ann Surg Oncol 2008;15:1008–14.
24. Li Y, Tian B, Yang J, Zhao L, Wu X, Ye SL, et al. Stepwise metastatic human hepatocellular carcinoma cell model system with multiple metastatic potentials established through consecutive *in vivo* selection and studies on metastatic characteristics. J Cancer Res Clin Oncol 2004;130:460–8.
25. Cui JF, Liu YK, Zhang LJ, Shen HL, Song HY, Dai Z, et al. Identification of metastasis candidate proteins among HCC cell lines by comparative proteome and biological function analysis of S100A4 in metastasis *in vitro*. Proteomics 2006;6:5953–61.
26. Llovet JM, Di Bisceglie AM, Bruix J, Kramer BS, Lencioni R, Zhu AX, et al. Design and endpoints of clinical trials in hepatocellular carcinoma. J Natl Cancer Inst 2008;100:698–711.
27. Li JC, Yang XR, Sun HX, Xu Y, Zhou J, Qiu SJ, et al. Up-regulation of Kruppel-like factor 8 promotes tumor invasion and indicates poor prognosis for hepatocellular carcinoma. Gastroenterology 2010;139:2146–57 e12.
28. Flohe L, Gunzler WA. Assays of glutathione peroxidase. Methods Enzymol 1984;105:114–21.
29. Mates JM, Perez-Gomez C, Nunez de Castro I. Antioxidant enzymes and human diseases. Clin Biochem 1999;32:595–603.

Published OnlineFirst April 18, 2012; DOI:10.1158/1078-0432.CCR-12-0183

30. Simon HU, Haj-Yehia A, Levi-Schaffer F. Role of reactive oxygen species (ROS) in apoptosis induction. Apoptosis 2000;5:415–8.
31. Schumacker PT. Reactive oxygen species in cancer cells: live by the sword, die by the sword. Cancer Cell 2006;10:175–6.
32. Pohl NM, Tong C, Fang W, Bi X, Li T, Yang W. Transcriptional regulation and biological functions of selenium-binding protein 1 in colorectal cancer *in vitro* and in nude mouse xenografts. PLoS One 2009;4:e7774.
33. Polyak K, Xia Y, Zweier JL, Kinzler KW, Vogelstein B. A model for p53-induced apoptosis. Nature 1997;389:300–5.
34. Beasley NJ, Leek R, Alam M, Turley H, Cox GJ, Gatter K, et al. Hypoxia-inducible factors HIF-1alpha and HIF-2alpha in head and neck cancer: relationship to tumor biology and treatment outcome in surgically resected patients. Cancer Res 2002;62:2493–7.
35. Carmeliet P, Dor Y, Herbert JM, Fukumura D, Brusselmans K, Dewerchin M, et al. Role of HIF-1alpha in hypoxia-mediated apoptosis, cell proliferation and tumour angiogenesis. Nature 1998;394:485–90.
36. Mizutani H. [Mechanism of DNA damage and apoptosis induced by anticancer drugs through generation of reactive oxygen species]. Yakugaku Zasshi 2007;127:1837–42.
37. Sinha BK, Mimnaugh EG. Free radicals and anticancer drug resistance: oxygen free radicals in the mechanisms of drug cytotoxicity and resistance by certain tumors. Free Radic Biol Med 1990;8:567–81.
38. Cao S, Durrani FA, Rustum YM. Selective modulation of the therapeutic efficacy of anticancer drugs by selenium containing compounds against human tumor xenografts. Clin Cancer Res 2004;10:2561–9.
39. Brozmanova J, Manikova D, Vlckova V, Chovanec M. Selenium: a double-edged sword for defense and offence in cancer. Arch Toxicol 2010;84:919–38.
40. Drake EN. Cancer chemoprevention: selenium as a prooxidant, not an antioxidant. Med Hypotheses 2006;67:318–22.
41. Lipinski B. Rationale for the treatment of cancer with sodium selenite. Med Hypotheses 2005;64:806–10.
42. Scarbrough PM, Mapuskar KA, Mattson DM, Gius D, Watson WH, Spitz DR. Simultaneous inhibition of glutathione- and thioredoxin-dependent metabolism is necessary to potentiate 17AAG-induced cancer cell killing via oxidative stress. Free Radic Biol Med 2012;52:436–43.

Journal of proteome research

Article

pubs.acs.org/jpr

Quantitative Proteomic Analysis Identified Paraoxonase 1 as a Novel Serum Biomarker for Microvascular Invasion in Hepatocellular Carcinoma

Cheng Huang,[†,#] Yuwei Wang,[†,#] Shengdong Liu,[†,#] Guangyu Ding,[†,#] Weiren Liu,[†] Jian Zhou,[†] Ming Kuang,[‡] Yuan Ji,[§] Tadashi Kondo,*[,∥] and Jia Fan*[,†]

[†]Liver Cancer Institute, Zhongshan Hospital and Shanghai Medical School, Fudan University, Key Laboratory for Carcinogenesis & Cancer Invasion, the Chinese Ministry of Education, Shanghai, China

[‡]Department of Hepatobiliary Surgery, The First Affiliated Hospital of Sun Yat-sen University, Guangzhou, China

[§]Department of Pathology, Zhongshan Hospital, Fudan University, Shanghai, China

[∥]Division of Pharmacoproteomics, National Cancer Center Research Institute, Tokyo, Japan

Supporting Information

ABSTRACT: This study aimed to identify serum biomarkers for microvascular invasion (MVI) in hepatocellular carcinoma (HCC). MVI is a histological sign of micrometastasis in the liver and is considered as one of the most powerful prognostic factors in HCC. The serum of HCC patients with different vascular invasion statuses was examined by iTRAQ-based proteomic profiling. The expression levels of 24 proteins were associated with the extent of vascular invasion in the pooled samples of 45 HCC cases. Western blot analyses in 90 HCC cases confirmed the correlation of the expression level of paraoxonase 1 (PON1) with the extent of vascular invasion. ELISA assays demonstrated the diagnostic utility of the PON1 level, with the area under curve values of 0.847 and 0.889 for the MVI and gross vascular invasion, respectively, relative to the patients without vascular invasion, in a cohort of 387 additional HCC cases. Immunohistochemistry revealed that PON1 expression in tumor cells was inversely correlated with the extent of vascular invasion in 200 additional HCC cases. In conclusion, using a proteomic approach, we found that serum PON1 was a novel diagnostic biomarker for MVI. The prognostic values of serum PON1 and its possible therapeutic applications are worth further investigation.

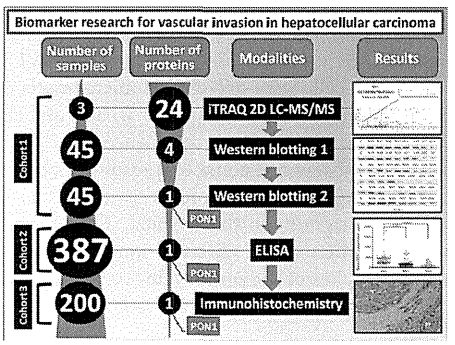

KEYWORDS: *hepatocellular carcinoma, paraoxonase 1, microvascular invasion*

INTRODUCTION

Hepatocellular carcinoma (HCC) is the sixth most common malignancy and the third leading cause of cancer death worldwide.[1] Although early diagnosis and surgical treatments have significantly improved overall survival rates, long-term survival rates remain poor because of high recurrence rates and metastasis, even with curative resection and transplantation.[2,3] Although clinical parameters correlate with prognosis and are used to determine the therapeutic strategies in HCC patients, the prediction of prognosis is far from satisfactory.[4,5] HCC patients often exhibit different clinical outcomes even when they are diagnosed at the same clinical stage. Therefore, more accurate prognostic modalities have long been desired for patients with HCC.

The presence of vascular invasion is regarded as one of the most important risk factors for poor prognosis because it is significantly associated with intrahepatic recurrence within two years after surgery.[6,7] Vascular invasion can be classified as gross vascular invasion (GVI) or microvascular invasion (MVI) on the basis of pathological observations, reflecting the degree of vascular invasion. The status of GVI and MVI represent malignant features of HCC and discrete prognoses for patients.[8] GVI can be diagnosed preoperatively using a radiological examination. GVI represents a late stage and is a crucial survival risk factor for hepatic resection. In contrast, MVI can currently be detected only by postresection histological examination, which greatly limits the utility of MVI when patients are given nonsurgical treatments, such as radiofrequency ablation, ethanol injection or transcatheter arterial chemoembolization.[7] Identification of proteins responsible for MVI may lead to novel prognostic modalities and therapeutic strategies.

In this study, we aimed to identify predictive serum proteins for MVI in HCC. Isobaric tags for relative and absolute quantitation (iTRAQ) and two-dimensional liquid chromatography–tandem mass spectrometry (2D LC–MS/MS) were used to examine the serum samples of HCC patients with

Received: December 15, 2012
Published: February 26, 2013

dx.doi.org/10.1021/pr3011815 | J. Proteome Res. 2013, 12, 1838–1846

different stages of vascular invasion.[9,10] We identified paraoxonase 1 (PON1) as a novel biomarker candidate for MVI. The correlation between PON1 and vascular invasion was validated by Western blotting and ELISA. Tissue localization and expression of PON1 were determined by immunohistochemistry. This is the first report concerning the clinical utility of PON1 for MVI in HCC.

MATERIALS AND METHODS

Study Patients and Sample Collection

This study included patients with HCC (n = 677) who underwent surgical treatment at the Zhongshan Hospital of Fudan University (Shanghai, China). The diagnosis of liver cancer was made by ultrasonography and dynamic computed tomography (CT) or magnetic resonance imaging (MRI), and the diagnosis of HCC was made by pathological examinations of the resected tissues after surgery. No patients had a biopsy prior to the operation or received preoperative treatments. Blood samples were drawn within one week of CT or MRI diagnosis and prior to surgical treatment.

The patients were classified into three groups based on their vascular invasion status: no vascular invasion (NVI), MVI, and GVI. The diagnosis of vascular invasion was made on the basis of established criteria.[7,8] The presence of MVI was diagnosed when tumor cells were detected in microvessels on microscopic observations by one pathologist (Y.J.) and one clinician (C.H.). In most cases, the presence or absence of MVI were so obvious that two reviewers had consistent results. Inconsistencies, if any, were resolved by discussion as is the usual procedure for pathologic diagnosis in the hospital. The presence of GVI was diagnosed when tumor thrombi were observed in the first or second branches of the portal veins on postoperative pathologic observations or by preoperative radiological tests, such as CT or MRI.

Serum samples were obtained from 90 patients between 2007 and 2008 (Cohort 1, Supporting Information Table S1) for proteomic assays and Western blotting. Those included 30 patients with NVI, 30 with MVI, and 30 with GVI. Another 387 serum samples from 147 patients with NVI, 196 with MVI, and 42 with GVI between 2010 and 2011 (Cohort 2, Supporting Information Table S2) were subjected to validation study by ELISA. Formalin-fixed paraffin-embedded tissue samples were obtained from a separate set of 200 patients between 2003 and 2006 (Cohort 3, Supporting Information Table S3) and examined by immunohistochemistry. Those included 77 patients with NVI, 80 with MVI, and 43 with GVI. The Ethics Committee of Fudan University approved this study, and all patients in this study provided written informed consent. The serum and tissue sample preparation procedures are described in the Supporting Information. The overview of the clinical samples and the study design is illustrated in Figure 1.

iTRAQ Coupled with 2D LC–MS/MS Analysis

To create quantitative protein expression profiles, an iTRAQ experiment was performed with 2D LC–MS/MS. Protein samples were digested and labeled with iTRAQ reagents as described previously.[11] Briefly, 45 serum samples from Cohort 1 were subjected to the proteomic study (NVI 1–15, MVI 1–15, GVI 1–15, Supporting Information Table S1). Equal volumes of serum from 15 patients with the same vascular invasion characteristics were mixed, and these three pooled samples were used for biomarker discovery (Figure 1). High-abundance plasma proteins, such as albumin, IgG and IgA, were

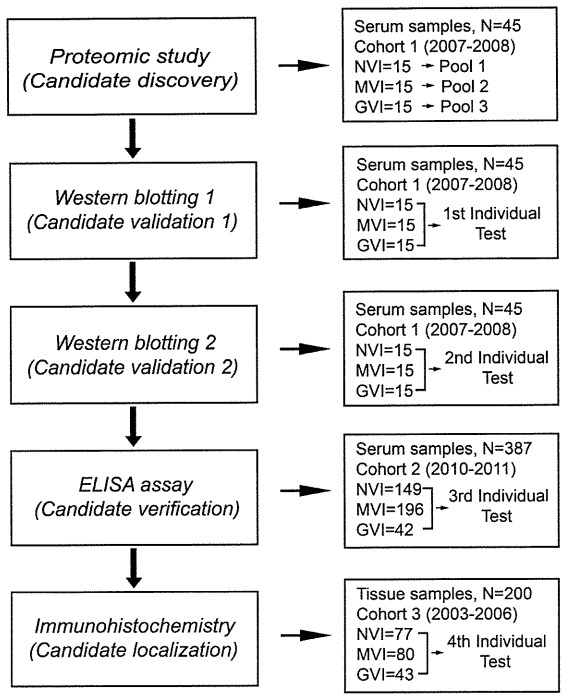

Figure 1. Overview of the study design for biomarker discovery, validation, and verification.

removed by the Human 14 Multiple Affinity Removal System (Agilent Technologies, Santa Clara, CA, USA), and then the samples were digested with trypsin and labeled with iTRAQ reagents (Applied Biosystems, Foster City, CA, USA). For iTRAQ analysis, peptides from the NVI group, as well as peptides from the MVI group and the GVI group, were labeled with iTRAQ tags 113, 114, and 115 from an 8-plex iTRAQ reagent kit, respectively. The three samples were then mixed, dried in a speed vacuum, and washed twice with 100 μL of Milli-Q water to remove any residual reagents. The iTRAQ reagent-labeled peptide mixtures were subsequently separated using a polysulfethyl A strong cation exchange column (5 μm, 300 Å, 0.5 × 23 mm; PolyLC Inc., Columbia, MD, USA) and a ZORBAX 300SB-C18 enrichment column (5 μm, 300 Å, 0.5 × 23 mm; Agilent Technologies). The ACQUITY Ultra Performance LC system (Waters, Milford, MA, USA) was coupled with a QSTAR XL mass spectrometer for electrospray analysis (Applied Biosystems/MDS SCIEX), and survey scans between m/z 400–1800 were acquired with up to six precursors selected for MS/MS analysis from m/z 100–2000 using dynamic exclusion. Fragmentation by rolling collision energy was optimized on the basis of the charge state and mass value of the precursor ions present. All measurements were performed in duplicate. Further methodological details are described in the Supporting Information.

Western Blot Analysis

Western blotting was performed to validate the correlation between the serum level of the identified proteins and the status of vascular invasion in HCC patients in Cohort 1 (Figure 1, Supporting Information Table S1). After diluting crude sera (without depleting abundant proteins) 10-fold with Milli-Q water, an equal volume of diluted serum (8 μL) and 2 μL of 5× loading buffer were loaded in each lane for 10 or 15% SDS-

dx.doi.org/10.1021/pr3011815 | J. Proteome Res. 2013, 12, 1838–1846

PAGE. The PageRuler Prestained Protein Ladder (Fermentas, USA) was used as a molecular weight marker. SDS-PAGE gels were run in duplicate to provide a gel for Coomassie blue staining for determining the amount of protein loaded for each sample (Supporting Information Figure S4). As no reliable internal control protein was available for Western blot analysis of the serum samples, a loading control sample was generated by pooling all of the samples from all groups in equal volumes for each gel. The separated proteins were transferred to polyvinylidene fluoride membranes (Millipore, Billerica, MA, USA). The membranes were blocked with 5% skim milk in TBS-Tween (25 mM Tris, 190 mM NaCl, 0.05% Tween 20, pH 7.5). Membranes were then incubated at 4 °C overnight with primary antibodies, such as those for amyloid A2 (SAA2; 1:1000, Abnova, Neihu District, Taipei City, Taiwan), clusterin isoform 1 (CLU; 1:1000, Abcam, Cambridge, MA, USA), complement factor B (CFB; 1:1000, Abcam), PON1 (1:1000, Abcam) and apolipoprotein A4 (APOA4; 1:1000, Abcam). After washing, the membranes were incubated at 25 °C for 1 h with the appropriate horseradish peroxidase-conjugated secondary antibody, washed, and developed with a chemiluminescence reagent (Thermo Fisher Scientific, Waltham, MA, USA). The signals from the bound antibodies were developed on films using chemiluminescence reagents (Thermo Fisher Scientific, Waltham, MA, USA). The films were then scanned by ImageScanner (Amersham Pharmacia Biotech), and the optical density of each band was measured with Quantity One (Bio-Rad) for semiquantitative analysis. The loading control sample in each gel was used as the standard for quantification.

Five proteins, SAA2, CLU, CFB, PON1, and APOA4, were initially validated in 45 cases (NVI 1–15, MVI 1–15, GVI 1–15, Supporting Information Table S1), and PON1 was further validated in an additional 45 serum samples (NVI 16–30, MVI 16–30, GVI 16–30, Figure 1, Supporting Information Table S1).

Measurement of Serum PON1 by ELISA

To establish the clinical utility of our findings, PON1 expression was examined in HCC patients in Cohort 2 (Figure 1, Supporting Information Table S2) by ELISA. A commercial ELISA kit (R&D Systems, Minneapolis, MN, USA) was used according to the manufacturer's recommendations. Briefly, 96-well microplates were coated with 100 μL of the monoclonal antibody to PON1 supplied with the ELISA kit (1 μg/mL) and incubated at 4 °C overnight. Nonspecific reactions were blocked with 1% bovine serum albumin. Patients' sera diluted with 10% neonatal calf serum were incubated for 2 h at 37 °C. Incubation with the detection antibody, biotinylated goat antihuman PON1 (600 ng/mL), was performed for 2 h at 37 °C, followed by the addition of 100 μL of a 1:200 dilution of streptavidin horseradish peroxidase for 20 min. Color development was achieved with 100 μL per well of 3,3,5,5-tetramethylbenzidine and hydrogen peroxide as a substrate, and sulfuric acid (1 mol/L) was added to stop the reaction. The optical density was measured at 450 nm and referenced to 570 nm on a Synergy 2 multimode plate reader (Biotek, Winooski, VT, USA). The concentrations of PON1 were obtained with a four-parameter logistic curve, fit to the standard value and multiplied by the dilution factor. All measurements were performed in duplicate.

Immunohistochemistry Assay

Expression and localization of PON1 in surgically resected tissues were immunohistochemically examined using paraffin-embedded tissue samples from HCC patients in Cohort 3 (Figure 1, Supporting Information Table S3). Paired 6-μm sections from the tumors and noncancerous margins (designated as tumor and peri-tumor tissues, respectively) for each patient were placed on the same slide to eliminate any experimental variation between different slide glasses. The antibody for PON1 (1:400, LifeSpan Biosciences Seattle, WA, USA) was used as a primary antibody. The pH of the citrate epitope retrieval buffer was adjusted to 6.0. Immunohistochemistry was performed using the two-step protocol recommended by the manufacturer (Novolink Polymer Detection System; Novocastra, Newcastle, U.K.). Negative control slides were treated in the same way, except that the primary antibody was omitted. Each slide was imaged using a Hitachi HV-C20A CCD camera (Hitachi, Tokyo, Japan) attached to a Leica DMLA light microscope (Leica Microsystems, Wetzlar, Germany).

The expression level of PON1 was scored on the basis of the intensity of staining of the cytoplasm of the cells over the entire section. The intensity of staining was quantified using a semiquantitative scoring system.[12] Briefly, the intensity of each slide was graded using a 4-point weighted score that was delimited as a semiquantitative scale: 1, extremely low; 2, low; 3, medium; and 4, high. Two pathologists (Y.J. and Y.Y.H.), without knowledge of the patient's characteristics, examined each slide independently, and the scores for all cases were compared to check for discrepancies. The final scores were assigned following discussion.

Statistical Analyses

Protein identification and quantification for the iTRAQ experiment was performed with the ProteinPilot software version 3.0 (Applied Biosystems, USA). The Paragon Algorithm in ProteinPilot software was used for peptide identification and isoform-specific quantification. MS/MS spectra were searched against the International Protein Index v3.45 human database (http://www.ebi.ac.uk/IPI/IPIhelp.html) with the following settings: trypsin digestion (semitryptic peptides allowed), methyl methanethiosulfonate modification of cysteines, iTRAQ 4-plex-labeled peptides, instrument QSTAR XL, *Homo sapiens*, no special factors, default iTRAQ isotope correction settings, quantification, bias correction, background correction, biological modifications and thorough ID parameters selected.

To minimize false-positive results, a strict cutoff for protein identification was applied with the unused ProtScore >1.3, which corresponds to a confidence limit of 95%, and at least two peptides with 95% confidence were considered for protein quantification. The resulting data set was auto-bias-corrected to remove any variations due to unequal mixing when combining different samples. Proteins with more than 1.2-fold or less than 0.8-fold differences between the groups were considered differentially expressed.

The software package SPSS v13.0 (SPSS Inc., Chicago, IL, USA) was used for statistical analyses. Qualitative variables were analyzed using Pearson's chi-squared and Fisher's exact tests, and quantitative variables were analyzed using ANOVA. Receiver operating characteristic (ROC) curve analysis was used to determine the diagnostic ability of the identified proteins associated with MVI versus GVI. All statistical tests were two-sided, and a P-value < 0.05 was considered statistically significant.

dx.doi.org/10.1021/pr3011815 | *J. Proteome Res.* 2013, 12, 1838–1846

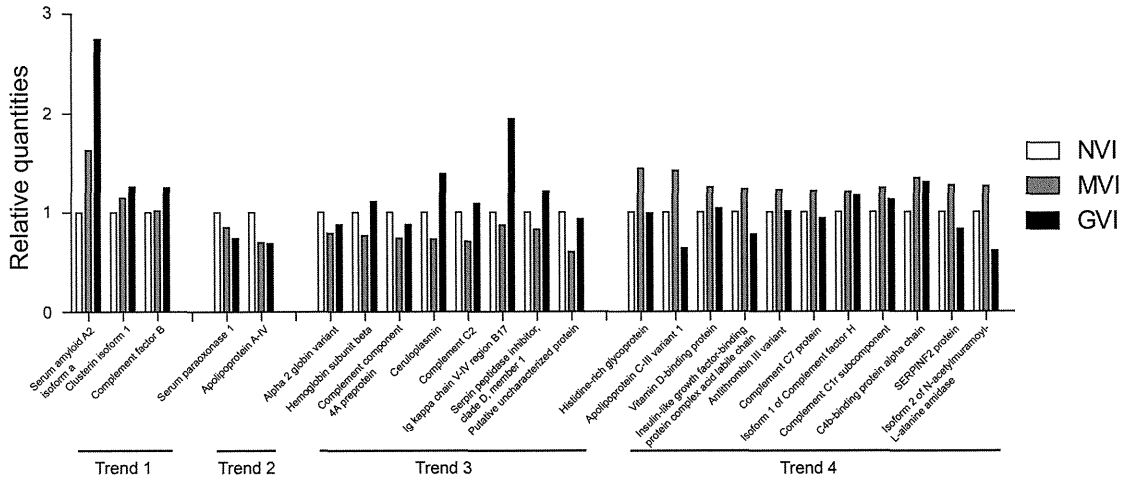

Figure 2. Relative quantities of 24 differentially expressed proteins by iTRAQ. The ratio for each protein for the no vascular invasion (NVI) group was given a value of 1. The proteins are organized according to the four trends that were observed. Trend 1: a gradual increase in protein levels with increased vascular invasion (serum amyloid A2 isoform a, clusterin isoform 1, and complement factor B). Trend 2: a gradual decrease in protein levels with increased vascular invasion (serum paraoxonase 1 and apolipoprotein A-IV). Trend 3: a decrease and then an increase in protein levels with increased vascular invasion (alpha 2 globin variant, hemoglobin subunit beta, complement component 4A preproprotein, ceruloplasmin, complement C2, Ig kappa chain V–IV region B17, serpin peptidase inhibitor, clade D (heparin cofactor), member 1, and putative uncharacterized protein DKFZp686H17246). Trend 4: an increase in protein levels followed by a decrease in protein levels with increased vascular invasion (histidine-rich glycoprotein, apolipoprotein C–III variant 1, vitamin D-binding protein, insulin-like growth factor-binding protein complex acid labile chain, antithrombin III variant, complement C7 protein, isoform 1 of complement factor H, complement C1r subcomponent, C4b-binding protein alpha chain, SERPINF2 protein, and isoform 2 of *N*-acetylmuramoyl-L-alanine amidase).

RESULTS

Quantification and Identification of Serum Proteins

Using iTRAQ and 2D LC–MS/MS, we compared the three pooled samples: serum samples from the patients with NVI, those with MVI, and those with GVI (Figure 1). We obtained quantitative data on 409 unique peptides and 73 proteins using iTRAQ and 2D LC–MS/MS (Supporting Information Tables S4, S5). Relative fold changes in concentration were calculated from the ratios of the iTRAQ reporter ion intensities in comparison between NVI and MVI, and between NVI and GVI. We found that 32 proteins showed differential expression in these two comparisons, with iTRAQ reporter ion intensities >1.2 or <0.8. The 32 proteins included 8 high-abundance proteins (isoform 1 of serum albumin, haptoglobin, IGHA1 protein, alpha-1-acid glycoprotein 1, alpha-1-acid glycoprotein 2, isoform 1 of the fibrinogen alpha chain, IGHM protein, and complement C3) that were supposed to be depleted by the immunodepletion column. As this could reflect the incomplete depletion, we excluded these 8 proteins from the following analysis. Compared with the serum samples that were pooled from patients with NVI, the levels of 11 proteins (vitamin D-binding protein, antithrombin III variant, histidine-rich glycoprotein, insulin-like growth factor-binding protein complex acid labile chain, serum amyloid A2 isoform a, apolipoprotein C–III variant 1, C4b-binding protein alpha chain, SERPINF2 protein, isoform 2 of *N*-acetylmuramoyl-L-alanine amidase, complement C1r subcomponent, and complement C7 protein) were increased, and the levels of 7 proteins (complement component 4A preproprotein, ceruloplasmin, apolipoprotein A-IV, hemoglobin subunit beta, alpha 2 globin variant, complement C2, and putative uncharacterized protein DKFZp686H17246) were decreased in the serum of patients with MVI (Supporting Information Table S6). Compared to those with NVI, in patients with GVI, some proteins (ceruloplasmin, complement factor B, clusterin isoform 1, serum amyloid A2 isoform a, C4b-binding protein alpha chain, serpin peptidase inhibitor, and Ig kappa chain V–IV region B17) were increased, and the levels of 5 proteins (apolipoprotein A-IV, insulin-like growth factor-binding protein complex acid labile chain, serum paraoxonase 1, apolipoprotein C–III variant 1, and isoform 2 of *N*-acetylmuramoyl-L-alanine amidase) were decreased (Supporting Information Table S6). The levels of serum amyloid A2 isoform a (SAA2), clusterin isoform 1 (CLU), and complement factor B (CFB) were positively correlated with the degree of vascular invasion, and the levels of serum paraoxonase 1 (PON1) and apolipoprotein A-IV (APOA4) were negatively correlated with the degree of vascular invasion (Figure 2, Supporting Information Table S6). We further validated the correlations between the serum levels of these 5 proteins and the vascular invasion status.

Validation of Serum Proteins by Western Blot Analysis

To confirm the correlation between the levels of SAA2, CLU, CFB, PON1, and APOA4 and the status of vascular invasion, 45 serum samples from the iTRAQ study (NVI 1–15, MVI 1–15, GVI 1–15, Supporting Information Table S1) were individually analyzed using Western blots (Supporting Information Figure S1). These experiments were conducted in duplicate, and the gel was stained with Coomassie brilliant blue for loading control analysis (Supporting Information Figure S4). SAA2 was not detected by Western blotting (data not shown). Among the other 4 proteins, only PON1 showed consistent data between the two experiments ($P < 0.05$, Figure 3A). In both iTRAQ and Western blotting, PON1 levels were decreased in MVI and decreased further in GVI, compared with the NVI group. Therefore, an additional 15 serum samples from each patient group (NVI 16–30, MVI 16–30, GVI 16–30, Supporting Information Table S1) were analyzed for PON1 concentration by Western blot (Figure 3B). In these assays, the

dx.doi.org/10.1021/pr3011815 | *J. Proteome Res.* 2013, 12, 1838–1846

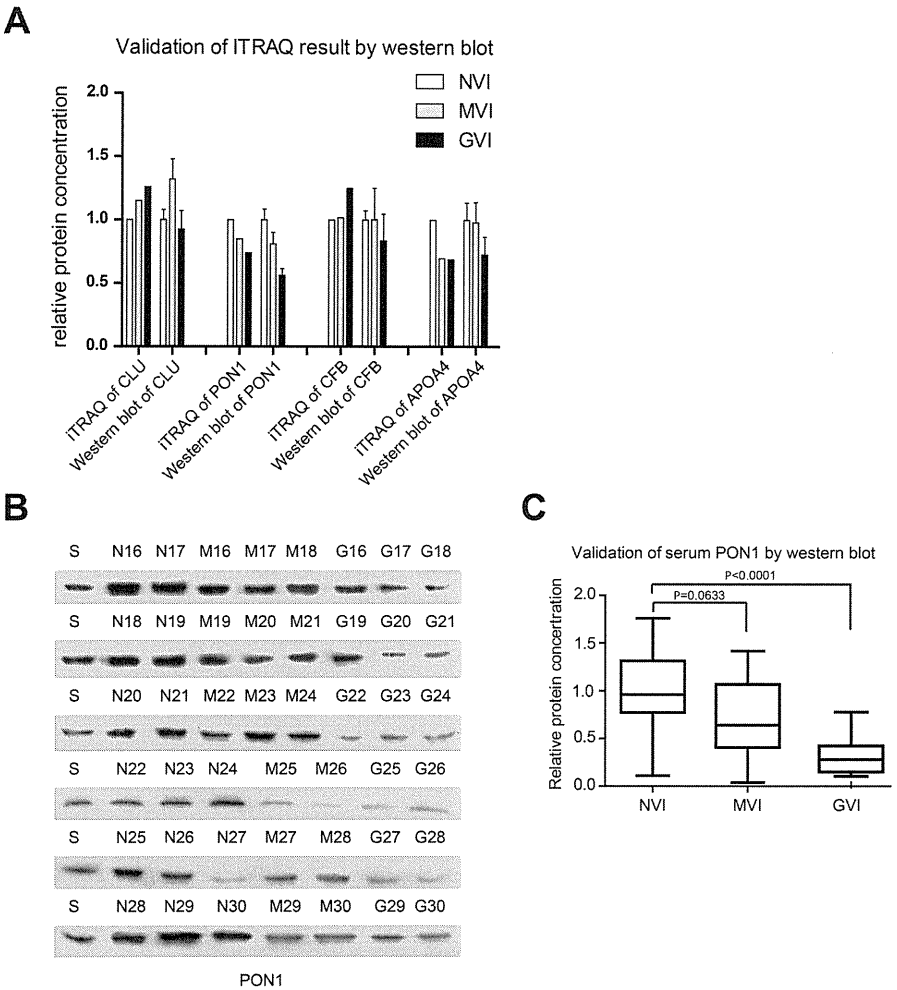

Figure 3. Validation of candidate biomarkers by Western blotting. (A) The average relative intensities of the proteins detected by iTRAQ and Western blot assays are normalized to the loading control for comparative studies. The results showed that only PON1 was consistent between two experiments ($P < 0.05$). (B) Serum PON1 level was further examined using Western blotting in 15 additional serum samples from each the patients with NVI (N16–N30), MVI (M16–M30) or GVI (G16–G30). (C) The average concentration of PON1 was 0.74-fold ($P = 0.0633$) and 0.39-fold ($P < 0.0001$) lower in the MVI and GVI groups, respectively, than the NVI group.

average concentration of PON1 was 0.74-fold ($P = 0.06$) and 0.39-fold ($P < 0.0001$) lower in samples of MVI and GVI, respectively, than in serum samples from patients with NVI (Figure 3C). As GVI is a more extended sign of vascular invasion of tumor cells than MVI, PON1 seemed to be responsible for vascular invasion.

Serum PON1 Validation by ELISA

We validated the correlation between PON1 expression and vascular invasion by ELISA in additional 387 HCC cases. Those cases included 147 cases with NVI, 196 cases with MVI and 42 cases with GVI (Cohort 2, Figure 1, Supporting Information Table S2). The mean concentrations of serum PON1 were 449, 158, and 89 pg/mL in the groups of NVI, MVI and GVI, respectively (Figure 4A). The PON1 concentration in the NVI group was significantly higher than in the MVI group ($P < 0.0001$) and GVI group ($P < 0.0001$). These observations were consistent with the data obtained by proteomic studies and Western blotting; the levels of PON1 expression in serum were inversely correlated with the degree of vascular invasion in HCC.

The diagnostic values of serum PON1 were evaluated by ROC curve analysis. The area under the curve (AUC) was 0.847 ($P < 0.001$) and 0.889 ($P < 0.001$) for MVI and GVI, respectively, relative to the patients with NVI (Figure 4B and C).

Immunohistochemical Characteristics

To explore the background of the inverse correlation between the PON1 expression and the vascular invasion, immunohistochemical studies were performed to localize PON1 in tumor and peri-tumor tissues. PON1 localized to the cytoplasm with a variety of staining intensities in HCC cells (Figure 5A). Homogeneous PON1 staining was observed in the cytoplasm of hepatocytes in peri-tumor tissues (Figure 5A). The expression levels of PON1 were evaluated according to a scoring system; representative photomicrographs of tumor and peri-tumor tissues showing the different staining patterns are presented in Figure 5B.

In tumor tissues, the PON1 expression levels were different between NVI, MVI, and GVI; the mean weighted scores were 2.04, 1.82, and 1.65 for the NVI, MVI, and GVI cases,

dx.doi.org/10.1021/pr3011815 | J. Proteome Res. 2013, 12, 1838–1846

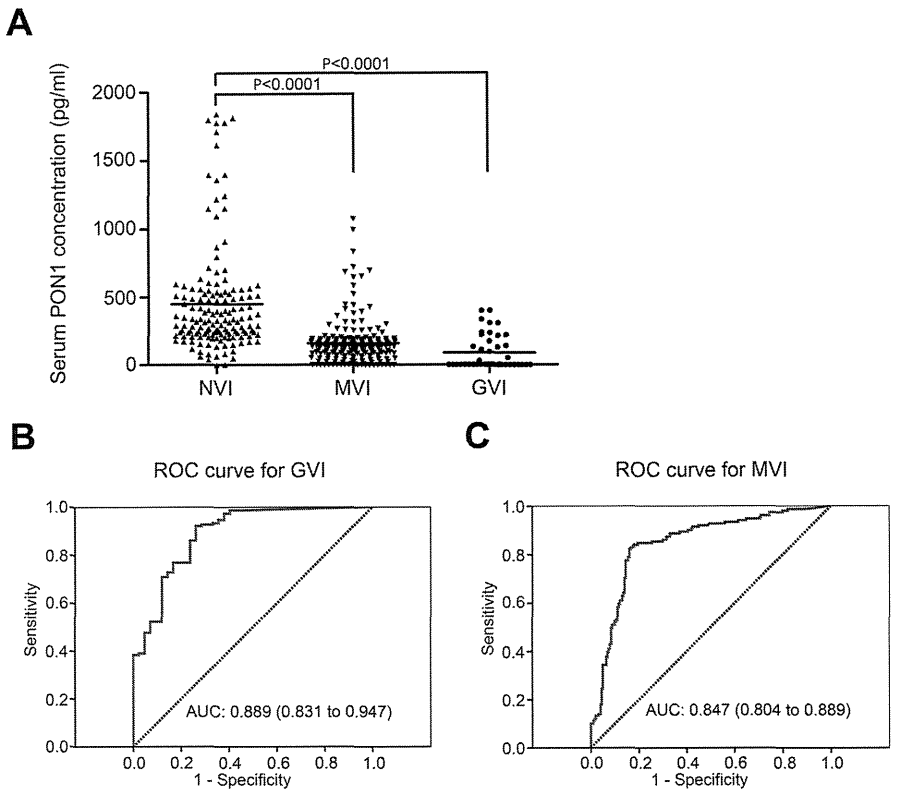

Figure 4. Validation of the diagnostic value of serum PON1 concentration in predicting vascular invasion by ELISA. (A) The serum PON1 concentration in 387 HCC patients (including 147 NVI, 196 MVI and 42 GVI patients) was determined using ELISA. The mean concentrations of serum PON1 in NVI, MVI, and GVI groups were 449, 158, and 89 pg/mL, respectively. Both MVI and GVI groups showed significantly lower levels of PON1 than the NVI group ($P < 0.0001$). (B) The receiver-operating characteristic curve (ROC curve) for the serum levels of PON1 in patients with GVI compared with patients with NVI. The area under each curve is 0.889 ($P < 0.001$). (C) The ROC curve for serum levels of PON1 in patients with MVI compared with patients with NVI. The area under each curve is 0.847 ($P < 0.001$).

respectively (Table 1). Tumor tissues from the NVI group showed the highest PON1 expression of all three groups ($P < 0.05$).

In peri-tumor tissues, PON1 expression was not different between the three groups: the mean weighted scores were 3.21, 3.24, and 3.23 for the NVI, MVI, and GVI cases, respectively (Table 1).

DISCUSSION

High rates of recurrence and metastasis are the major causes of the poor prognosis of HCC after surgery. Knowing the prognosis allows the best selection of presently available therapies for HCC. However, current clinicopathologic factors, such as histological classification and tumor size, cannot accurately predict the prognosis of HCC patients.[13−15] Thus, novel modalities to assess the malignant potential of tumor cells and prognostic biomarkers have long been sought.[15] Vascular invasion is a sign of the spread of cancer cells via the vasculature, which may be a key mechanism underlying intrahepatic recurrence and metastasis.[7,8] Thus, we can consider vascular invasion as an indirect evaluation of prognosis. GVI can be diagnosed preoperatively using radiological examination, and the degree of GVI was highly correlated with a poor prognosis and considered as a prognostic biomarker.[13] In contrast, the detection of MVI is achieved only by histological observations in resected tissues, and the features of MVI cannot be examined without invasive treatments. As the presence of MVI is a sign of early metastasis, the detection of MVI before surgery would help select the proper therapeutic modalities.[16] Moreover, the identification of MVI will expand the indications for liver transplantation in HCC. Liver transplantation has long been accepted as a curative treatment option for HCC patients within the Milan criteria, which are based on the number and size of tumors.[17] Recent studies indicated that the criteria could be expanded for patients without vascular invasion; the patients with multiple or larger tumors may achieve acceptable 5-year survival rates.[5,18] Therefore, by assessing MVI prior to the surgical operation, we will detect more patients who are likely to benefit from liver transplantation. With this background, we aimed to identify serum biomarker candidates to detect MVI.

Comprehensiveness is generally reciprocal to throughput in biomarker studies. Although proteomic modalities enable highly sensitive protein identification in a quantitative manner, it is difficult to examine a large number of samples in a short period. For validation, it is desirable to use a tool that allows parallel examinations of a limited number of molecules, to survey more samples. Moreover, the cost for examinations should be reduced as much as possible, if clinical application is desired. In this study, we initially used three pooled samples for proteomic studies to identify the biomarker candidates using iTRAQ and 2D LC−MS/MS. Then, we achieved candidate validation using a less complex method, Western blotting, for the first screening in 45 samples and for the second screening in another 45 samples. Finally, we examined the clinical

dx.doi.org/10.1021/pr3011815 | J. Proteome Res. 2013, 12, 1838−1846

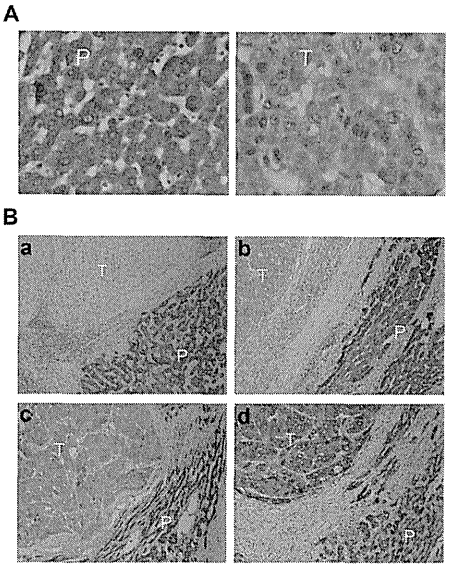

Figure 5. Immunohistochemical staining for PON1 in hepatocellular carcinoma tumors and peri-tumor tissues. (A) PON1 localized to the cytoplasm both in HCC cells and peri-tumor hepatocytes. (B) Tumor cells stained for PON1 in photomicrographs (a), (b), (c) and (d) were scored as 1, 2, 3 and 4, respectively. Peri-tumor hepatocytes in the four representative photomicrographs were all scored as 4. T represents tumor tissue and P represents peri-tumor tissue.

significance of the biomarker candidate by a higher-throughput and less expensive method, ELISA, in an additional 387 cases and evaluated the clinical utilities of the candidates with ROC curve analysis. For verification, we performed immunohistochemistry in the other 200 cases. We initially used a smaller number of samples and a more sophisticated method, and we then examined the results in a larger number of samples and a simpler method. This study design is a role model for biomarker research.

PON1 is a calcium-dependent hydrolase protein synthesized mainly in the liver and secreted into the circulatory system.[19] The systemic immunohistochemical survey of PON1 expression in normal tissues and organs revealed that PON1 was unique to normal hepatocytes and skin (The Human Protein Atlas ver 10.0, http://www.proteinatlas.org/). We speculate that serum levels of PON1 might reflect PON1 expression changes in tumor or nontumor tissues during the progression of liver cancer.[20,21] The immunohistochemical study demonstrated that PON1 expression in tumor tissues inversely is correlated with vascular invasion status, whereas its expression in peri-tumor tissues shows no significant association (Table 1). This finding suggests that the serum concentration of PON1 may be modulated primarily by PON1 expression in the tumor tissue rather than nontumoral hepatic tissues. These observations are consistent with a previous report, where 35 gene signatures for MVI and GVI were identified; the mRNA level of PON1 was elevated in tumors with NVI compared to tumors with MVI or GVI.[22] While there were suggestive observations to correlate the PON1 levels in tissues and serum, further investigation on the functional significances of aberrant regulation of PON1 in tissue and serum should be required before clinical applications.

Serum PON1 has been implicated in cell damage and chronic inflammation in the liver. In chronic liver disease, PON1 levels in serum and hepatic tissue correlate with the degree of liver damage.[23,24] As an important antiatherosclerotic factor, PON1 has the capacity to prevent oxidation of low-density lipoprotein (LDL), maintain the normal function of endothelial cells, inhibit the adhesion of leukocytes (especially monocytes and macrophages), and reduce chronic inflammation of the vascular wall.[19,25−27] Because chronic inflammation and leukocyte adhesion are the hallmarks of tumor vascularization and abnormalities in tumor vessels play a crucial role in the process of tumor invasion and metastasis,[28,29] the anti-inflammatory and vessel normalization roles of PON1 could underlie the inverse correlation between serum PON1 concentration and HCC vascular invasion. The molecular mechanisms underlying the down-regulation of PON1 in HCC with vascular invasion are worth further investigation.

Clinical applications of serum PON1 may require additional investigation. First, our results were obtained only from HBV-induced HCC; therefore, the HCC patients with other etiologies, such as chronic HCV-infection and nonviral diseases, should be included in the further validation studies. Allelic heterogeneity for PON1 in the human population has recently been reported in studies of cardiovascular disease and metabolic syndrome.[30−32] It is worth investigating whether genotype differences of PON1 exist in HCC patients and whether these differences correlate with tumor invasion and metastasis. Second, the optimal cutoff value should be determined in a larger number of serum samples. Any single marker may not be sufficient for the final decision about therapeutic strategy, and all clinical and pathological information should be considered when using biomarker data. We intend to continue performing a multicenter validation study. Third, the expression of PON1 was reported in many types of cancers such as lung cancer,[33] breast cancer,[34] colorectal cancer,[35] ovarian cancer,[36] endometrial cancer,[37] gastric cancer,[38] and pancreatic cancer.[39] In these cancers, the vascular invasions are observed in the

Table 1. Weighted Scores for the Immunohistochemical Staining of PON1 in HCC Tumor and Peri-tumor Tissues

		number (%) of patients of different weighted score					
tissue localization[a]	vascular invasion status[a]	1	2	3	4	mean weighted score[b]	*P*-value[c]
T	NVI (*N* = 77)	18 (23.4)	40 (51.9)	17 (22.1)	2 (2.6)	2.04 ± 0.08	0.031
	MVI (*N* = 80)	34 (42.5)	28 (35.0)	16 (20.0)	2 (2.5)	1.82 ± 0.09	
	GVI (*N* = 43)	22 (51.2)	15 (34.9)	5 (11.6)	1 (2.3)	1.65 ± 0.12	
P	NVI (*N* = 77)	0 (0.0)	3 (3.9)	5 5(71.4)	19 (24.7)	3.21 ± 0.06	0.929
	MVI (*N* = 80)	0 (0.0)	3 (3.8)	55 (68.7)	22 (27.5)	3.24 ± 0.06	
	GVI (*N* = 43)	0 (0.0)	2 (4.7)	29 (67.4)	12 (27.9)	3.23 ± 0.08	

[a]Abbreviations: T, hepatic tumor cells; P, peri-tumor hepatocytes; NVI, no vascular invasion; MVI, microvascular invasion; GVI, gross vascular invasion. [b]Values are given as means ± SEM. [c]*P*-value < 0.05 was considered statistically significant. *P*-values were calculated using the ANOVA test.

dx.doi.org/10.1021/pr3011815 | *J. Proteome Res.* 2013, 12, 1838−1846

patients at the developed clinical stage. Therefore, PON1 may generally contribute to the vascular invasion of tumor cells. This hypothesis seems to be attractive, and further expression study on PON1 should be performed in the different types of malignancies.

Our present study has a technical limitation in terms of the coverage of proteome by iTRAQ. The number of serum proteins could be increased by extensive fractionations by affinity columns, size exclusion columns and ion exchange columns, and by the use of mass spectrometry-based, antibody-based or gel-based applications with higher sensitivity. We do not consider that PON1 is the only and best biomarker protein for MVI. Our study clearly demonstrated the presence of biomarker proteins such as PON1 for MVI, and the additional biomarker candidates should be further investigated using the other proteomics modalities.

In conclusion, taking advantage of proteomic modalities and considering global and focused experiments, we identified serum PON1 concentration as a novel preoperative biomarker for MVI in HCC. Serum PON1 concentration can be potentially included in the patient selection standards for more intense follow-up, adjuvant treatment or liver transplantation. Further investigation of the origin of serum PON1 and the mechanisms underlying the inverse correlation between serum PON1 and vascular invasion will allow deep insights into HCC biology.

■ ASSOCIATED CONTENT

Supporting Information

Supporting tables and figures. Table S1: Clinical and Demographic Characteristics of 90 HCC Patients in Cohort 1. Table S2: Clinical and Demographic Characteristics of 387 HCC Patients in Cohort 2. Table S3: Clinical and Demographic Characteristics of 200 HCC Patients in Cohort 3. Table S4: List of 409 Peptides Identified in HCC Serum Samples by iTRAQ. Table S5: List of 73 Proteins Identified in HCC Serum Samples by iTRAQ. Table S6: Differentially Expressed Proteins Identified in HCC Serum Samples by iTRAQ. Figure S1: Forty five serum samples from the iTRAQ study were further analyzed using Western blot. Figure S2: SDS-PAGE was used to evaluate the immunodepletion of samples by Affinity Removal System Columns. Figure S3: Sequence identification and quantification of representative iTRAQ-labeled peptides of complement factor B, serum paraoxonase 1, clusterin isoform 1, and apolipoprotein A-IV. Figure S4: Coomassie brilliant blue was used to stain the SDS-PAGE gels prior to transfer of the proteins to membranes for Western blot assays. This material is available free of charge via the Internet at http://pubs.acs.org.

■ AUTHOR INFORMATION

Corresponding Author

*Tel: 0086-21-64037181 (J.F.). Fax: 0086-21-64037181 (J.F.). E-mail: fan.jia@zs-hospital.sh.cn (J.F.); proteomebioinformatics@gmail.com (T.K.).

Author Contributions

#C. Huang, Y. Wang, S. Liu, and G. Ding contributed equally to this work.

Notes

The authors declare no competing financial interest.

■ ACKNOWLEDGMENTS

We thank the patients and clinicians at the Liver Cancer Institute and Zhongshan Hospital, Fudan University, for their contributions to this study. This work is financially supported by grants from the National Natural Science Foundation of China (No. 30600605), the Major Program of NSFC (No. 81030038), and the National Key Sci-Tech Project of China (2008ZX10002-019).

■ ABBREVIATIONS

HCC, hepatocellular carcinoma; MVI, microvascular invasion; GVI, gross vascular invasion; NVI, no vascular invasion; PON1, paraoxonase 1; iTRAQ, isobaric tags for relative and absolute quantitation; 2D LC–MS/MS, two-dimensional liquid chromatography–tandem mass spectrometry; SAA2, amyloid A2; CLU, clusterin isoform 1; CFB, complement factor B; APOA4, apolipoprotein A4; ROC, receiver operating characteristic curve; HBsAg, hepatitis B surface antigen; ALB, albumin; AFP, α-fetoprotein; ALT, alanine transaminase; TB, total bilirubin

■ REFERENCES

(1) Parkin, D. M.; Bray, F.; Ferlay, J.; Pisani, P. Global cancer statistics, 2002. *Ca—Cancer J. Clin.* **2005**, *55* (2), 74–108.

(2) Poon, R. T. Differentiating early and late recurrences after resection of HCC in cirrhotic patients: implications on surveillance, prevention, and treatment strategies. *Ann. Surg. Oncol.* **2009**, *16* (4), 792–4.

(3) Llovet, J. M.; Ricci, S.; Mazzaferro, V.; Hilgard, P.; Gane, E.; Blanc, J. F.; de Oliveira, A. C.; Santoro, A.; Raoul, J. L.; Forner, A.; Schwartz, M.; Porta, C.; Zeuzem, S.; Bolondi, L.; Greten, T. F.; Galle, P. R.; Seitz, J. F.; Borbath, I.; Haussinger, D.; Giannaris, T.; Shan, M.; Moscovici, M.; Voliotis, D.; Bruix, J. Sorafenib in advanced hepatocellular carcinoma. *N. Engl. J. Med.* **2008**, *359* (4), 378–90.

(4) Dudek, K.; Kornasiewicz, O.; Remiszewski, P.; Kobryn, K.; Ziarkiewicz-Wroblewska, B.; Gornicka, B.; Zieniewicz, K.; Krawczyk, M. Impact of tumor characteristic on the outcome of liver transplantation in patients with hepatocellular carcinoma. *Transplant. Proc.* **2009**, *41* (8), 3135–7.

(5) Mazzaferro, V.; Llovet, J. M.; Miceli, R.; Bhoori, S.; Schiavo, M.; Mariani, L.; Camerini, T.; Roayaie, S.; Schwartz, M. E.; Grazi, G. L.; Adam, R.; Neuhaus, P.; Salizzoni, M.; Bruix, J.; Forner, A.; De Carlis, L.; Cillo, U.; Burroughs, A. K.; Troisi, R.; Rossi, M.; Gerunda, G. E.; Lerut, J.; Belghiti, J.; Boin, I.; Gugenheim, J.; Rochling, F.; Van Hoek, B.; Majno, P. Predicting survival after liver transplantation in patients with hepatocellular carcinoma beyond the Milan criteria: a retrospective, exploratory analysis. *Lancet Oncol.* **2009**, *10* (1), 35–43.

(6) Bruix, J.; Llovet, J. M. Major achievements in hepatocellular carcinoma. *Lancet* **2009**, *373* (9664), 614–6.

(7) Roayaie, S.; Blume, I. N.; Thung, S. N.; Guido, M.; Fiel, M. I.; Hiotis, S.; Labow, D. M.; Llovet, J. M.; Schwartz, M. E. A system of classifying microvascular invasion to predict outcome after resection in patients with hepatocellular carcinoma. *Gastroenterology* **2009**, *137* (3), 850–5.

(8) Lim, K. C.; Chow, P. K.; Allen, J. C.; Chia, G. S.; Lim, M.; Cheow, P. C.; Chung, A. Y.; Ooi, L. L.; Tan, S. B. Microvascular invasion is a better predictor of tumor recurrence and overall survival following surgical resection for hepatocellular carcinoma compared to the Milan criteria. *Ann. Surg.* **2011**, *254* (1), 108–13.

(9) Gstaiger, M.; Aebersold, R. Applying mass spectrometry-based proteomics to genetics, genomics and network biology. *Nat. Rev. Genet.* **2009**, *10* (9), 617–27.

(10) Wepf, A.; Glatter, T.; Schmidt, A.; Aebersold, R.; Gstaiger, M. Quantitative interaction proteomics using mass spectrometry. *Nat. Methods* **2009**, *6* (3), 203–5.

dx.doi.org/10.1021/pr3011815 | *J. Proteome Res.* 2013, 12, 1838–1846

(11) Jin, G. Z.; Li, Y.; Cong, W. M.; Yu, H.; Dong, H.; Shu, H.; Liu, X. H.; Yan, G. Q.; Zhang, L.; Zhang, Y.; Kang, X. N.; Guo, K.; Wang, Z. D.; Yang, P. Y.; Liu, Y. K. iTRAQ-2DLC-ESI-MS/MS based identification of a new set of immunohistochemical biomarkers for classification of dysplastic nodules and small hepatocellular carcinoma. *J. Proteome Res.* **2011**, *10* (8), 3418–28.

(12) Yiu, G. K.; Chan, W. Y.; Ng, S. W.; Chan, P. S.; Cheung, K. K.; Berkowitz, R. S.; Mok, S. C. SPARC (secreted protein acidic and rich in cysteine) induces apoptosis in ovarian cancer cells. *Am. J. Pathol.* **2001**, *159* (2), 609–22.

(13) Qin, L. X.; Tang, Z. Y. Recent progress in predictive biomarkers for metastatic recurrence of human hepatocellular carcinoma: a review of the literature. *J. Cancer Res. Clin. Oncol.* **2004**, *130* (9), 497–513.

(14) Ye, Q. H.; Qin, L. X.; Forgues, M.; He, P.; Kim, J. W.; Peng, A. C.; Simon, R.; Li, Y.; Robles, A. I.; Chen, Y.; Ma, Z. C.; Wu, Z. Q.; Ye, S. L.; Liu, Y. K.; Tang, Z. Y.; Wang, X. W. Predicting hepatitis B virus-positive metastatic hepatocellular carcinomas using gene expression profiling and supervised machine learning. *Nat. Med.* **2003**, *9* (4), 416–23.

(15) Villanueva, A.; Hoshida, Y.; Battiston, C.; Tovar, V.; Sia, D.; Alsinet, C.; Cornella, H.; Liberzon, A.; Kobayashi, M.; Kumada, H.; Thung, S. N.; Bruix, J.; Newell, P.; April, C.; Fan, J. B.; Roayaie, S.; Mazzaferro, V.; Schwartz, M. E.; Llovet, J. M. Combining clinical, pathology, and gene expression data to predict recurrence of hepatocellular carcinoma. *Gastroenterology* **2011**, *140* (5), 1501–12 e2.

(16) Sumie, S.; Kuromatsu, R.; Okuda, K.; Ando, E.; Takata, A.; Fukushima, N.; Watanabe, Y.; Kojiro, M.; Sata, M. Microvascular invasion in patients with hepatocellular carcinoma and its predictable clinicopathological factors. *Ann. Surg. Oncol.* **2008**, *15* (5), 1375–82.

(17) Freeman, R. B., Jr. Transplantation for hepatocellular carcinoma: The Milan criteria and beyond. *Liver Transplant.* **2006**, *12* (11 Suppl 2), S8–13.

(18) Roayaie, S.; Frischer, J. S.; Emre, S. H.; Fishbein, T. M.; Sheiner, P. A.; Sung, M.; Miller, C. M.; Schwartz, M. E. Long-term results with multimodal adjuvant therapy and liver transplantation for the treatment of hepatocellular carcinomas larger than 5 centimeters. *Ann. Surg.* **2002**, *235* (4), 533–9.

(19) Precourt, L. P.; Amre, D.; Denis, M. C.; Lavoie, J. C.; Delvin, E.; Seidman, E.; Levy, E. The three-gene paraoxonase family: physiologic roles, actions and regulation. *Atherosclerosis* **2011**, *214* (1), 20–36.

(20) Ferre, N.; Marsillach, J.; Camps, J.; Mackness, B.; Mackness, M.; Riu, F.; Coll, B.; Tous, M.; Joven, J. Paraoxonase-1 is associated with oxidative stress, fibrosis and FAS expression in chronic liver diseases. *J. Hepatol.* **2006**, *45* (1), 51–9.

(21) Kedage, V.; Muttigi, M. S.; Shetty, M. S.; Suvarna, R.; Rao, S. S.; Joshi, C.; Prakash, M. Serum paraoxonase 1 activity status in patients with liver disorders. *Saudi J. Gastroenterol.* **2010**, *16* (2), 79–83.

(22) Minguez, B.; Hoshida, Y.; Villanueva, A.; Toffanin, S.; Cabellos, L.; Thung, S.; Mandeli, J.; Sia, D.; April, C.; Fan, J. B.; Lachenmayer, A.; Savic, R.; Roayaie, S.; Mazzaferro, V.; Bruix, J.; Schwartz, M.; Friedman, S. L.; Llovet, J. M. Gene-expression signature of vascular invasion in hepatocellular carcinoma. *J. Hepatol.* **2011**, *55* (6), 1325–31.

(23) Keskin, M.; Dolar, E.; Dirican, M.; Kiyici, M.; Yilmaz, Y.; Gurel, S.; Nak, S. G.; Erdinc, S.; Gulten, M. Baseline and salt-stimulated paraoxonase and arylesterase activities in patients with chronic liver disease: relation with disease severity. *Intern. Med. J.* **2009**, *39* (4), 243–8.

(24) Marsillach, J.; Camps, J.; Ferre, N.; Beltran, R.; Rull, A.; Mackness, B.; Mackness, M.; Joven, J. Paraoxonase-1 is related to inflammation, fibrosis and PPAR delta in experimental liver disease. *BMC Gastroenterol.* **2009**, *9*, 3.

(25) Bouman, H. J.; Schomig, E.; van Werkum, J. W.; Velder, J.; Hackeng, C. M.; Hirschhauser, C.; Waldmann, C.; Schmalz, H. G.; ten Berg, J. M.; Taubert, D. Paraoxonase-1 is a major determinant of clopidogrel efficacy. *Nat. Med.* **2011**, *17* (1), 110–6.

(26) Wheeler, J. G.; Keavney, B. D.; Watkins, H.; Collins, R.; Danesh, J. Four paraoxonase gene polymorphisms in 11212 cases of coronary heart disease and 12786 controls: meta-analysis of 43 studies. *Lancet* **2004**, *363* (9410), 689–95.

(27) Zabirnyk, O.; Liu, W.; Khalil, S.; Sharma, A.; Phang, J. M. Oxidized low-density lipoproteins upregulate proline oxidase to initiate ROS-dependent autophagy. *Carcinogenesis* **2010**, *31* (3), 446–54.

(28) Coussens, L. M.; Werb, Z. Inflammation and cancer. *Nature* **2002**, *420* (6917), 860–7.

(29) Carmeliet, P.; Jain, R. K. Principles and mechanisms of vessel normalization for cancer and other angiogenic diseases. *Nat. Rev. Drug Discovery* **2011**, *10* (6), 417–27.

(30) Gupta, N.; Singh, S.; Maturu, V. N.; Sharma, Y. P.; Gill, K. D. Paraoxonase 1 (PON1) polymorphisms, haplotypes and activity in predicting cad risk in North-West Indian Punjabis. *PLoS One* **2011**, *6* (5), e17805.

(31) Bhattacharyya, T.; Nicholls, S. J.; Topol, E. J.; Zhang, R.; Yang, X.; Schmitt, D.; Fu, X.; Shao, M.; Brennan, D. M.; Ellis, S. G.; Brennan, M. L.; Allayee, H.; Lusis, A. J.; Hazen, S. L. Relationship of paraoxonase 1 (PON1) gene polymorphisms and functional activity with systemic oxidative stress and cardiovascular risk. *JAMA, J. Am. Med. Assoc.* **2008**, *299* (11), 1265–76.

(32) Kordi-Tamandani, D. M.; Hashemi, M.; Sharifi, N.; Kaykhaei, M. A.; Torkamanzehi, A. Association between paraoxonase-1 gene polymorphisms and risk of metabolic syndrome. *Mol. Biol. Rep.* **2012**, *39* (2), 937–43.

(33) Elkiran, E. T.; Mar, N.; Aygen, B.; Gursu, F.; Karaoglu, A.; Koca, S. Serum paraoxonase and arylesterase activities in patients with lung cancer in a Turkish population. *BMC Cancer* **2007**, *7*, 48.

(34) Bobin-Dubigeon, C.; Jaffre, I.; Joalland, M. P.; Classe, J. M.; Campone, M.; Herve, M.; Bard, J. M. Paraoxonase 1 (PON1) as a marker of short term death in breast cancer recurrence. *Clin. Biochem.* **2012**, *45* (16–17), 1503–5.

(35) Balci, H.; Genc, H.; Papila, C.; Can, G.; Papila, B.; Yanardag, H.; Uzun, H. Serum lipid hydroperoxide levels and paraoxonase activity in patients with lung, breast, and colorectal cancer. *J. Clin. Lab. Anal.* **2012**, *26* (3), 155–60.

(36) Camuzcuoglu, H.; Arioz, D. T.; Toy, H.; Kurt, S.; Celik, H.; Erel, O. Serum paraoxonase and arylesterase activities in patients with epithelial ovarian cancer. *Gynecol. Oncol.* **2009**, *112* (3), 481–5.

(37) Arioz, D. T.; Camuzcuoglu, H.; Toy, H.; Kurt, S.; Celik, H.; Erel, O. Assessment of serum paraoxonase and arylesterase activity in patients with endometrial cancer. *Eur. J. Gynaecol. Oncol.* **2009**, *30* (6), 679–82.

(38) Akcay, M. N.; Yilmaz, I.; Polat, M. F.; Akcay, G. Serum paraoxonase levels in gastric cancer. *Hepatogastroenterology* **2003**, *50* (Suppl 2), cclxxiii–cclxxv.

(39) Akcay, M. N.; Polat, M. F.; Yilmaz, I.; Akcay, G. Serum paraoxonase levels in pancreatic cancer. *Hepatogastroenterology* **2003**, *50* (Suppl 2), ccxxv–ccxxvii.

dx.doi.org/10.1021/pr3011815 | *J. Proteome Res.* 2013, 12, 1838–1846

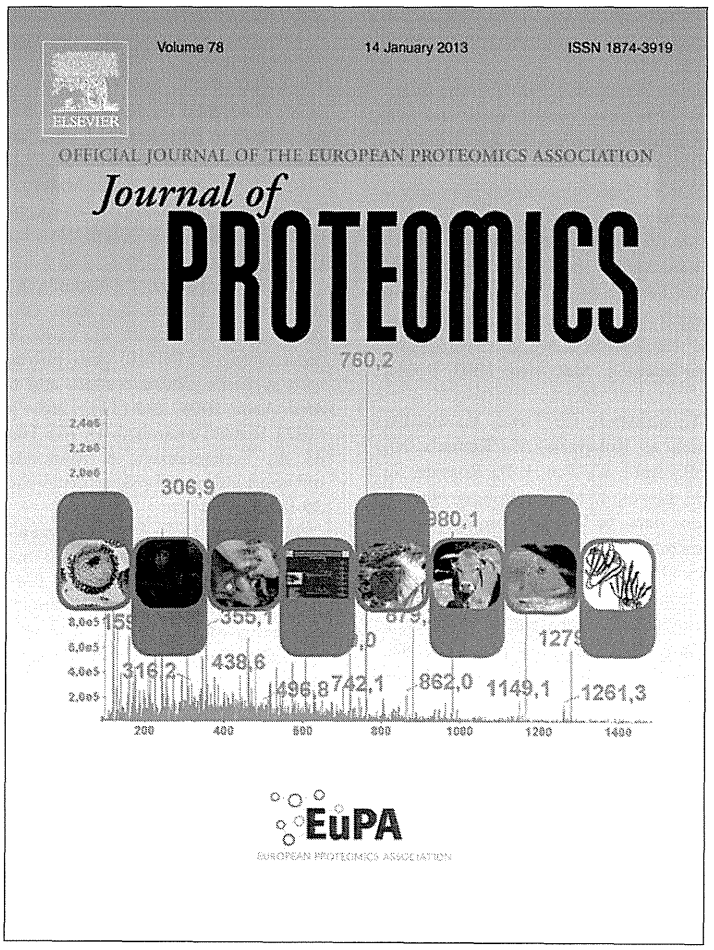

JOURNAL OF PROTEOMICS 78 (2013) 362–373

Available online at www.sciencedirect.com

SciVerse ScienceDirect

www.elsevier.com/locate/jprot

Proteomic identification of the macrophage-capping protein as a protein contributing to the malignant features of hepatocellular carcinoma☆

Kazuya Kimura[a], *Hidenori Ojima*[b], *Daisuke Kubota*[a], *Marimu Sakumoto*[a], *Yukiko Nakamura*[a,c], *Tsuyoshi Tomonaga*[c], *Tmoo Kosuge*[d], *Tadashi Kondo*[a,*]

[a]*Division of Pharmacoproteomics, National Cancer Center Research Institute, Tokyo, Japan*
[b]*Division of Molecular Pathology, National Cancer Center Research Institute, Tokyo, Japan*
[c]*Laboratory of Proteome Research, National Institute of Biomedical Innovation, Tokyo, Japan*
[d]*Hepatobiliary and Pancreatic Surgery Division, National Cancer Center Hospital, Tokyo, Japan*

ARTICLE INFO

Article history:
Received 8 August 2012
Accepted 8 October 2012
Available online 17 October 2012

Keywords:
Hepatocellular carcinoma
Venous invasion
Biomarker
Two-dimensional difference gel electrophoresis
Macrophage-capping protein (CapG)

ABSTRACT

Hepatocellular carcinoma (HCC) is one of the most deadly cancers worldwide. We performed a proteomic study to understand the molecular mechanisms underlying metastasis in HCC. Among the 3491 protein spots observed by two-dimensional difference gel electrophoresis (2D-DIGE), we found that 197 and 88 protein spots had statistically significant differences in intensity between tumor and non-tumor tissues and between the tumors with and without vascular invasion, respectively. Mass spectrometry was used to identify the proteins corresponding to those protein spots. We found that compared to tumor tissues without vascular invasion, those with vascular invasion showed markedly upregulated expression of the macrophage-capping protein (CapG). The association of increased CapG expression with vascular invasion in the tumor tissues was confirmed by western blotting. CapG expression levels were equal for non-tumor tissues and tumor tissues without venous invasion, as assessed by 2D-DIGE and western blotting. Silencing of CapG reduced tumor invasion without affecting the proliferation of the HCC cells. These observations suggested that CapG is involved in the process of metastasis by promoting the invasiveness of tumor cells. It may therefore be worth investigating the clinical usefulness of CapG as a biomarker in risk-stratification therapy and as a therapeutic target in HCC.

1. Introduction

Hepatocellular carcinoma (HCC) is the third leading cause of cancer-related death and is an increasingly prevalent clinical problem worldwide. The prognosis of patients in the late stages of the disease is extremely poor [1]. Although molecular-targeted therapies are in development, they have not yet been established, and surgery is still the first choice for complete cure. A poor clinical outcome in HCC patients is attributable to the highly vascular nature of HCC tumors, which potentiates the tumor cells to disseminate to other parts of the liver. The presence of vascular invasion, which remarkably reflects the vascular invasiveness of the HCC, reflects intrahepatic metastases, which cause early

☆ Potential conflict of interest: Nothing to report.

* *Corresponding author at:* Division of Pharmacoproteomics, National Cancer Center Research Institute, 5-1-1 Tsukiji, Chuo-ku, Tokyo 104-0045, Japan. Tel.: +81 3 3542 2511x3004; fax: +81 3 3547 5298.
E-mail address: takondo@ncc.go.jp (T. Kondo).

1874-3919/$ – see front matter © 2012 Elsevier B.V. All rights reserved.
http://dx.doi.org/10.1016/j.jprot.2012.10.004

recurrences [2,3]. Thus, vascular invasion is one of the major clinically important features of metastatic HCCs, and its molecular background is worth investigating for developing improved therapeutic strategies. Novel therapies to prevent recurrence following surgical resection have been challenged, and the use of anti-cancer reagents to prevent recurrence has been reported, including the mTOR inhibitor [4], sorafenib [5], interferon-alpha [6,7], acyclic retinoids [8], and dimeric beta peptides [9]. By assessing the potential for venous invasiveness of tumor cells, we may be able to optimize the use of anti-recurrence drugs in HCC patients, and more importantly, we will be able to identify novel therapeutic targets.

Much effort has been devoted to molecular studies on the early recurrence of HCCs. Proteomic approaches have identified proteins with unique expression in primary tumor tissues from patients who later experienced recurrence [10]. Proteomic studies on HCCs have identified novel proteins, including the APC-binding protein EB1 [11], which can be used as a predictor for HCC recurrence by immunohistochemical analysis. Extensive global expression studies for vascular invasion have also involved mRNA [12] and micro RNA [13] analyses, and several promising biomarker candidates and therapeutic targets have been identified. The clinical usefulness of identifying gene products is of great interest for clinical application in HCC patients.

In this study, we examined the proteins associated with vascular invasion in the primary tumor tissues of the HCC. Although vascular invasion is one of the predictive biomarkers for early recurrence in HCC, its proteomic backgrounds have not been well examined. Using two-dimensional difference gel electrophoresis (2D-DIGE) and our original large-format electrophoresis apparatus, we examined tumor tissues from patients with different levels of vascular invasion. We identified the macrophage-capping protein (CapG) as an important protein associated with vascular invasion and validated the results by proteomics analysis involving antibodies and in vitro studies.

2. Materials and methods

2.1. Clinical samples

This study included 26 primary tumor tissue samples from HCC patients and 19 non-tumor liver tissue samples. The non-tumor tissue samples included 2 liver tissue samples of individuals with hepatitis, 2 liver tissue samples of individuals with liver cirrhosis, and 15 normal liver tissue samples. Tumor tissues were obtained from 12 HCC patients who had vascular invasion and from 14 who did not. The clinicopathological observations for the HCC patients are summarized in Table 1, and the clinicopathological data of the individual HCC patients are available in Supplementary Table 1. Tumor and non-tumor tissues were obtained at the time of surgery. The specimens were snap-frozen in liquid nitrogen and stored at −80 °C until use. Clinical staging (TNM system) was determined on the basis of diagnostic imaging criteria. None of these patients received anti-neoplastic therapy before surgery. The patients underwent curative surgery at the National Cancer Center Hospital. This study was approved by the ethics committee of the National Cancer Center, and written informed consent was obtained from all the patients.

Table 1 – Summary of clinico-pathological data of HCC patients.

	All cases (n=26)	Venous invasion		p value
		Positive (n=12)	Negative (n=14)	
Age				0.04453
Median	67.5	57	71	
Virus type				
HBV	12	9	3	0.00429
HCV	12	3	9	
NBNC	2	0	2	
Gender				0.51463
Male	19	8	11	
Female	17	4	3	
Histological grade				0.0014
Well differentiated	5	6	0	
Moderately	15	6	9	
Poorly	6	0	5	
Edmondson grade				0.00016
I	6	0	6	
II	14	6	8	
III	6	6	0	

2.2. Protein extraction

Proteins were extracted from surgically resected tissues as previously described [14]. In brief, the frozen tissues were pulverized in liquid nitrogen using metal beads (Multi-beads shocker; Yasui-kikai, Osaka, Japan). The tissues were then treated with urea lysis buffer (2 M thiourea, 7 M urea, 3% CHAPS and 1% Triton X-100). After centrifugation, the supernatant was recovered as a soluble protein fraction and stored at −80 °C until use.

2.3. Two-dimensional difference gel electrophoresis

A protein expression profile was created as previously described [14]. In brief, an internal control sample was prepared by mixing an equal amount of a small portion of all the individual samples. Fifteen micrograms of individual samples and the internal control sample were labeled with the Cy5 and Cy3 fluorescent dyes (CyDye DIGE fluor saturation dyes; GE, Uppsala, Sweden), respectively, according to the manufacturer's instructions. The differently labeled protein samples were mixed together, divided into 3 samples, and separated using two-dimensional gel electrophoresis. First-dimension separation was achieved using an IPG dry strip gel, with an isoelectric focusing range of 4 to 7 (24 cm length), and Multiphor II (GE). Protein samples were applied to the IPG gels using a reswelling method and were separated by isoelectric focusing using the IPG gels. Second-dimension separation was performed using SDS-PAGE overnight with our original large-format gel apparatus [14], with a separation distance of 33 cm and a circulating-water cooling system. After gel electrophoresis, gels sandwiched by low-fluorescent glass plates were scanned using a laser scanner (Typhoon Trio,

GE), and Cy5 and Cy3 images were obtained by single scans. The Cy5 spot intensity was normalized with Cy3 for all protein spots by using the image analysis software Progenesis SameSpot (Non-linear Dynamics, Newcastle, UK). For preparative purposes, 100 μg of the protein sample was labeled with the Cy3 fluorescent dye and separated as described above. The protein spots of interest were matched between the images of analytical and preparative gels and recovered onto 96-well plates from the preparative gels by using our original spot-recovery machine (Molecular Hunter; AsOne, Osaka, Japan) [14]. The protein spots recovered were stored at 4 °C until use.

2.4. Statistical analysis

The protein expression profile data were exported as an XML file from the Progenesis SameSpot software and were imported to the data-mining software Expressionist (GeneData, Basel, Switzerland).

2.5. Mass spectrometric protein identification

The proteins were extracted as peptides from the protein spots by in-gel digestion as previously reported [14]. In brief, the protein spots recovered were washed extensively with acetonitrile and ammonium bicarbonate minimum solution and treated with trypsin (Promega, Madison, WI) at 37 °C overnight. Tryptic digests were recovered from the gel pieces, concentrated under vacuum, and resolubilized with 0.1% trifluoroacetic acid. The final tryptic digests were subjected to liquid chromatography with the Paradigm MS4 dual solvent delivery system (Michrom BioResources, Auburn, CA) and an LTQ linear ion trap MS (Thermo Electron, San Jose, CA) equipped with a nano-electrospray ion source (AMR, Tokyo, Japan). The Mascot software (version 2.3.02; Matrix Science Inc., Boston, MA) was used to search for the mass of the peptide ion peaks against the SWISS-PROT database (*Homo sapiens*, 471,472 sequences in the Sprot_57.5 fasta file). The MASCOT search parameters were as follows: the peptide tolerance was 1.3 Da, and the MS/MS tolerance was 1 Da (monoisotopic mass). Fixed modifications of carbamidomethylation and variable modifications of oxidation, 2+ and 3+ peptide charge were selected, and up to 3 missed trypsin cleavages were allowed. Proteins with a Mascot score of 34 or more were used for protein identification.

2.6. Western blotting

All the 45 protein samples used for 2D-DIGE were examined by western blotting. In brief, protein samples were separated by SDS-PAGE with Criterion TGX Precast Gels (Bio-Rad, Hercules, CA). Five micrograms of each protein was separated by SDS-PAGE, and the separated proteins were transferred to a nitrocellulose membrane. The protein transfer was achieved using a conventional western blotting buffer system. After blocking with skimmed milk for 1 h, the membrane was reacted with anti-CapG antibodies from Protreintech (Chicago, IL; 1:500 dilution) or GenWay (San Diego, CA; 1:1000 dilution) overnight. Subsequently, the membranes treated with the antibody from Proteintech or GenWay were treated with the second antibody against rabbit IgG (GE; 1:2000 dilution) or chicken IgY (Santa Cruz Biotechnology, Santa Cruz, CA; 1:4000), respectively. The membranes were processed by enhanced chemiluminescence (ECL Prime, GE). After the membranes were scanned with LAS-3000 (FujiFilm, Tokyo, Japan), they were stained with 0.2% Ponceau S and 1% acetic acid (Sigma Aldrich, St. Louis, MO), and the intensity of the protein bands was measured by the ImageQuant software (GE). The intensity of individual protein bands was normalized with the intensity of the lane on an identical membrane in the SDS-PAGE/western blots.

2.7. RNA interference, cell growth assay, and invasion assay

The human HLE cell line was obtained from the Health Science Research Resources Bank (Tokyo, Japan) and cultured in RPMI 1640 medium supplemented with 10% fetal bovine serum (Gibco BRL, Auckland, NZ). The target mRNA sequences for small interfering RNA (siRNA) were as follows for human CAPG: 5′-CAAGAGAACCAGGGCGUCUUCUUCU-3′ (siRNA 1) and 5′-GG CAAUGAGUCUGACCUCUUCAUGA-3′ (siRNA 2). A Stealth RNAi Negative Control Duplex (control siRNA), which was designed to minimize sequence homology to any known vertebrate transcript, was used as the control. The CAPG-specific (siRNA1 and siRNA2) and control siRNAs were purchased from Invitrogen (Carlsbad, CA). A total of 1×10^5 cells were seeded into each well of a 6-well tissue culture plate (Costar, Cambridge, MA). The cell monolayer was washed the next day with pre-warmed sterile phosphate-buffered saline (PBS). The cells were transfected with the siRNAs using Lipofectamine™ 2000 Reagent (Invitrogen) according to the manufacturer's protocol. Then, HLE cells were seeded at a density of 1.5×10^3 cells/well in 96-well plates. The cells were transfected the next day with the siRNAs, and after 3–5 days of culture, cell viability was measured using a cell counting kit (Dojindo Laboratories, Kumamoto, Japan) according to the manufacturer's instructions. After 2 h of incubation at 37 °C, the optical density was measured at a wavelength of 450 nm using a microplate reader. For protein extraction, the cells were washed twice with PBS, treated with 10% TCA for 30 min on ice, and scraped off into a tube. The cell pellet was incubated for 30 min in urea lysis buffer and centrifuged at 15,000 rpm for 30 min. The supernatant was recovered, and the protein concentration was measured with a protein assay kit (Bio-Rad, Hercules, CA). The samples recovered were subjected to western blotting to monitor the expression level of CaPG by using anti-CaPG antibody (Proteintech). Cell invasion was assayed in 24-well Biocoat Matrigel invasion chambers (8 μm; Becton Dickinson, Bedford, MA) according to the manufacturer's protocol. Briefly, the cells were treated with siRNAs, and on the following day, 1×10^4 cells were plated in the upper chamber. The bottom chamber contained 10% FBS as a chemoattractant. Forty-eight hours later, the noninvasive cells were removed with a cotton swab. The cells that migrated through the membrane and stuck to the lower surface of the membrane were fixed with methanol and stained with the Diff Quik stain (Sysmex, Hyogo, Japan). For quantification, the cells were photographed under a microscope at ×200 magnification and counted in 3 fields of triplicate membranes.

3. Results

3.1. 2D-DIGE with internal control samples

We created protein expression profiles using 2D-DIGE. Fig. 1A illustrates the design of the 2D-DIGE experiments. Cy5-labeled individual protein samples were mixed with a Cy3-labeled internal control sample and separated by 2D-PAGE. By normalizing the Cy5 intensity with the Cy3 control for all protein spots, the gel-to-gel variation could be compensated. This protocol enabled the examination of all 45 samples in this study by using 2 fluorescent dyes.

To observe larger numbers of protein spots, we used our original large-format 2D apparatus [14]. Fig. 1B shows a typical 2D image of the internal control sample. We assessed the

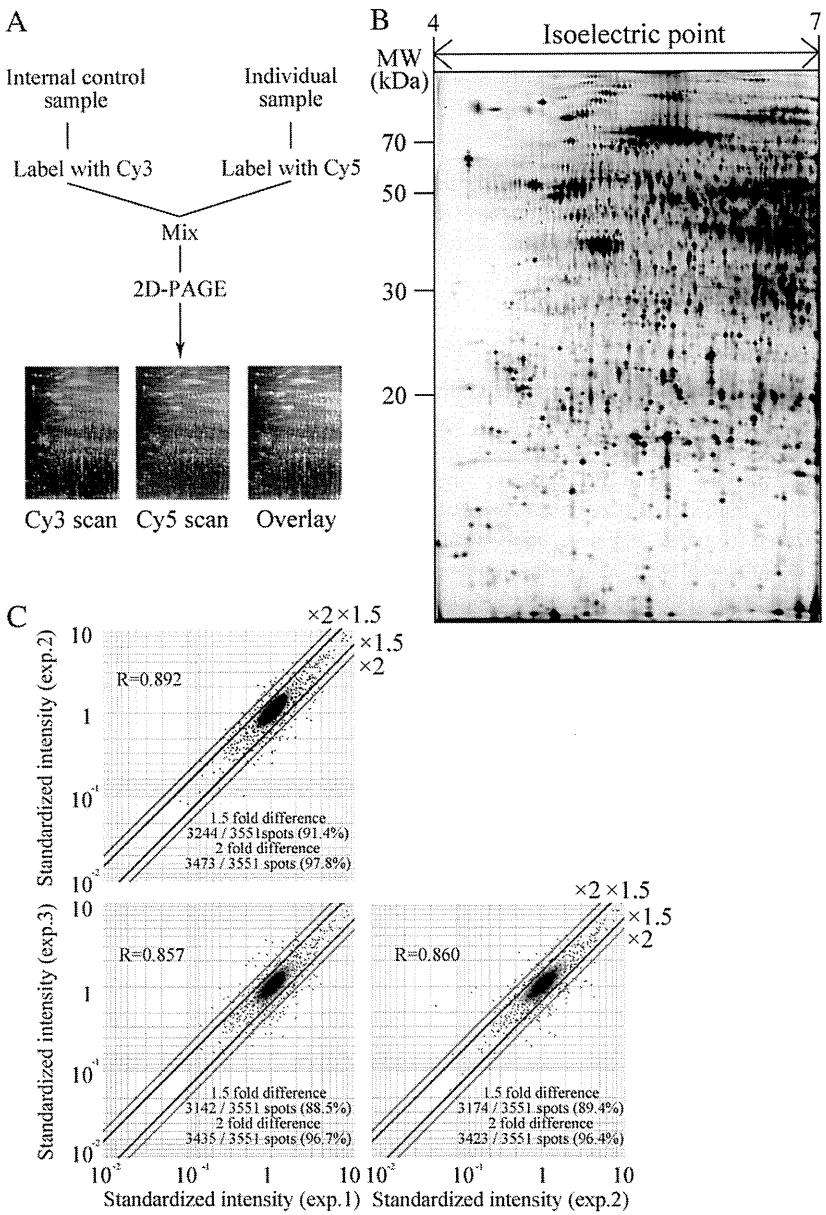

Fig. 1 – Overview of the 2D-DIGE experiments. A: Sample preparation for the 2D-DIGE experiments. The internal control and the individual samples were labeled with Cy3 and Cy5 fluorescent dyes, respectively. They were mixed together and separated by 2D-PAGE. After gel electrophoresis, the gel was scanned with a laser scanner. The spot intensity of the Cy5-labeled protein samples was normalized with the Cy3-labeled sample in the same gel. B: A typical 2D image of a Cy3-labeled internal control sample. The proteins were separated according to their isoelectric points and molecular weights. In total, 3491 protein spots were observed in a single gel. The enlarged 2D image is provided in Supplementary Figs. 1–3. C: Scattergrams show the system reproducibility. One sample was examined 3 times, and the intensities of individual protein spots were compared among the 3 experiments. Note that the correlation coefficient was at least 0.860, and the intensities of more than 88.5% of the protein spots had less than 1.5-fold differences.

system reproducibility of our proteomic study by examining the same sample 3 times. Fig. 1C shows the scattergrams for the triplicate experiments. The intensities of at least 88.5% of the scattered protein spots indicated less than 1.5-fold differences, and the relative coefficients were at least 0.857. The high reproducibility may be due to the use of the internal

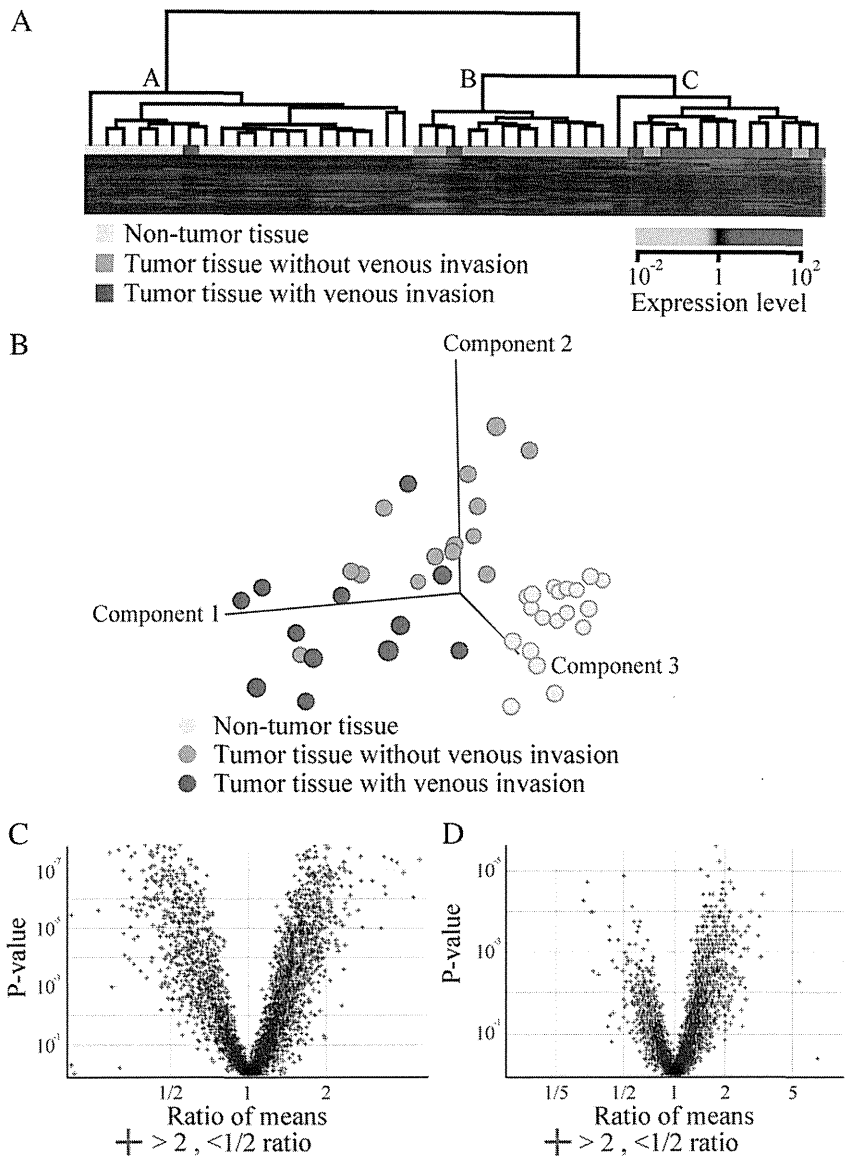

Fig. 2 – Overall features of the proteome examined by unsupervised classification. A: Samples were grouped by hierarchical clustering on the basis of the intensity of all 3491 protein spots. Note that the samples were mainly divided into 3 groups; most samples in tree A were non-tumor tissue samples, and the majority of samples in trees B and C were tumor tissue samples. The samples in trees B and C were tumor samples without and with vascular invasion, respectively. B: Samples were plotted in a three-dimensional space by principal component analysis based on the intensities of 3491 protein spots. Note that the samples were mainly divided into non-tumor tissues and tumor tissues. Tumor tissues were apparently divided into 2 groups, those with or those without vascular invasion. C: The 3491 protein spots were plotted as a function of fold differences and p-values, comparing non-tumor tissues with tumor tissues by a volcano plot. The ratio of means was calculated by dividing the averaged intensities of the tumor tissue samples with the non-tumor tissue samples. We identified 197 protein spots with statistically significant differences (fold difference>2; $p<0.05$) in intensity. D: The protein spots were plotted as a function of the fold differences and p-values on comparing the tumor tissues with and without portal vein invasion by using a volcano plot. The mean ratio was calculated by dividing the average intensity of the tumor tissue samples with vascular invasion with those with no vascular invasion. Note that 88 protein spots with statistically significant differences in intensity (fold difference>2; $p<0.05$) were identified. The spot intensities of all protein spots are summarized in Supplementary Table 2. The localization of the protein spots assessed by mass spectrometric protein analysis is shown in Supplementary Figs. 1–3.

control sample and the large format gels. We conducted the proteomic studies with this level of reproducibility.

3.2. *Overall features of the proteome data generated by 2D-DIGE*

First, we examined the overall features of the proteome by unsupervised classification. The protein samples were grouped by hierarchical clustering according to the intensity of 3491 protein spots (Fig. 2A). The normalized intensity of 3491 protein spots across 45 samples is summarized in Supplementary Table 2. The samples were divided into 3 major groups: trees A, B, and C. Tree A was mostly composed of the 19 non-tumor tissue samples, except for 1 tumor tissue sample. The majority of the samples in tree B were the 11 tumor tissues with no vascular invasion, except for 1 tumor tissue. Ten of the 13 samples in tree C were the tumor tissue samples with vascular invasion, and the rest were those without. Principal component analysis provided similar results (Fig. 2B). Overall, the non-tumor samples were discriminated from the tumor tissue samples, and the tumor tissues were separated according to the status of the vascular invasion.

We examined volcano plots to identify the proteins that were possibly responsible for the difference in the features between the tumor and non-tumor tissues and between the tumor tissues with vascular invasion and those without (Fig. 2C and D). The protein spots that exhibited a statistically significant difference (>2-fold difference; $p<0.05$) in intensity were selected for protein identification by mass spectrometry. In the comparison between the tumor and non-tumor tissue groups, we found that 197 protein spots met these criteria; 80 and 117 spots showed higher and lower intensities, respectively, in the tumor tissue group than in the non-tumor tissue (Fig. 2C). On comparing the tumor tissues with and without vascular invasion, we also found that there were 88 protein spots that met the abovementioned criteria; 72 and 16 spots had higher and lower intensities, respectively, in the tumor tissues with vascular invasion than in those without vascular invasion (Fig. 2D). The locations of these protein spots are shown in Supplementary Figs. 1 and 2.

We found that 23 protein spots were commonly identified in the following 2 sets of comparisons: the first being between non-tumor and tumor tissues and the second between tumor tissues with vascular invasion and those without. Among these 23 spots, 12 had a higher intensity in the tumor tissues than in the non-tumor tissues, and even higher intensities were observed in the tumor tissues with vascular invasion than in those without (Figs. 3 and 4). However, 6 protein spots had lower intensities in the tumor tissue group than in the non-tumor tissue group, and they showed lower expression in the vascular invasion-positive tumor tissues than in the vascular invasion-negative tumor tissues (Figs. 3 and 4).

3.3. *Mass spectrometric protein identification of the protein spots with differing intensities between the sample groups*

The 197 protein spots with differing intensities between the non-tumor tissues and tumor tissues were analyzed by mass spectrometry (Fig. 3). These 197 protein spots corresponded to 103 unique gene products. The list of identified proteins and the peptide data to support the protein identification are shown in Supplementary Tables 3 and 4, respectively. The locations of the 197 protein spots are shown in Supplementary Fig. 1. The 80 protein spots with higher intensities in the tumor tissue group corresponded to 54 unique gene products (Fig. 3A), and the 117 with lower intensities, to 64 unique gene products (Fig. 3B).

The 88 protein spots with differing intensities between the tumor tissues with vascular invasion and those without were also analyzed by mass spectrometry (Fig. 4). The list of the identified proteins and the peptide data to support the protein identification are shown in Supplementary Tables 5 and 6, respectively. The locations of the 88 protein spots are shown in Supplementary Fig. 2. The 88 protein spots corresponded to 55 unique gene products. The 72 protein spots with higher intensities in the tumor tissues with vascular invasion corresponded to 47 unique gene products, and the 16 with lower intensities, to 13 unique gene products.

In addition to the protein spots with significant intensity differences between sample groups, we determined the identities of 310 protein spots. The list of the 310 proteins identified, and the peptide data to support protein identification are shown in Supplementary Tables 5 and 6, respectively. The locations of these 310 protein spots are shown in Supplementary Fig. 3.

3.4. *Overexpression of CapG in the tumor tissues with vascular invasion*

We focused on CapG. The expression level of CapG was higher in the tumor tissues with vascular invasion than in those without (Fig. 4); however, there were no significant differences observed between the tumor and non-tumor tissues (Fig. 3). These observations suggest that CapG is specifically associated with the progression of the cancer rather than carcinogenesis in HCC. In a previous proteomic study, we found that the expression of CapG was correlated with a poor response to treatment with gemcitabine in cholangiocarcinoma, and confirmed its prognostic usefulness by immunohistochemical analysis; the patients with CapG-positive primary tumors had worse prognoses than those who did not [15]. CapG overexpression has been reported in a range of malignancies [16–21]. However, an association between CapG expression and vascular invasion in HCC had not yet been reported. These observations led us to further examine the expression of CapG in HCC.

3.5. *Validation of the expression levels of CapG using antibodies*

We validated the expression of CapG using western blotting with 2 specific antibodies against CapG to confirm the results of the 2D-DIGE experiments. Using both antibodies, the expression level of CapG was seen to be significantly higher in the tumor tissues with vascular invasion than in those without vascular invasion and in the non-tumor liver tissues (Fig. 5). In contrast, no significant differences were observed between the non-tumor tissues and tumor tissues (Fig. 5). Overall, these results were consistent with those obtained by 2D-DIGE.

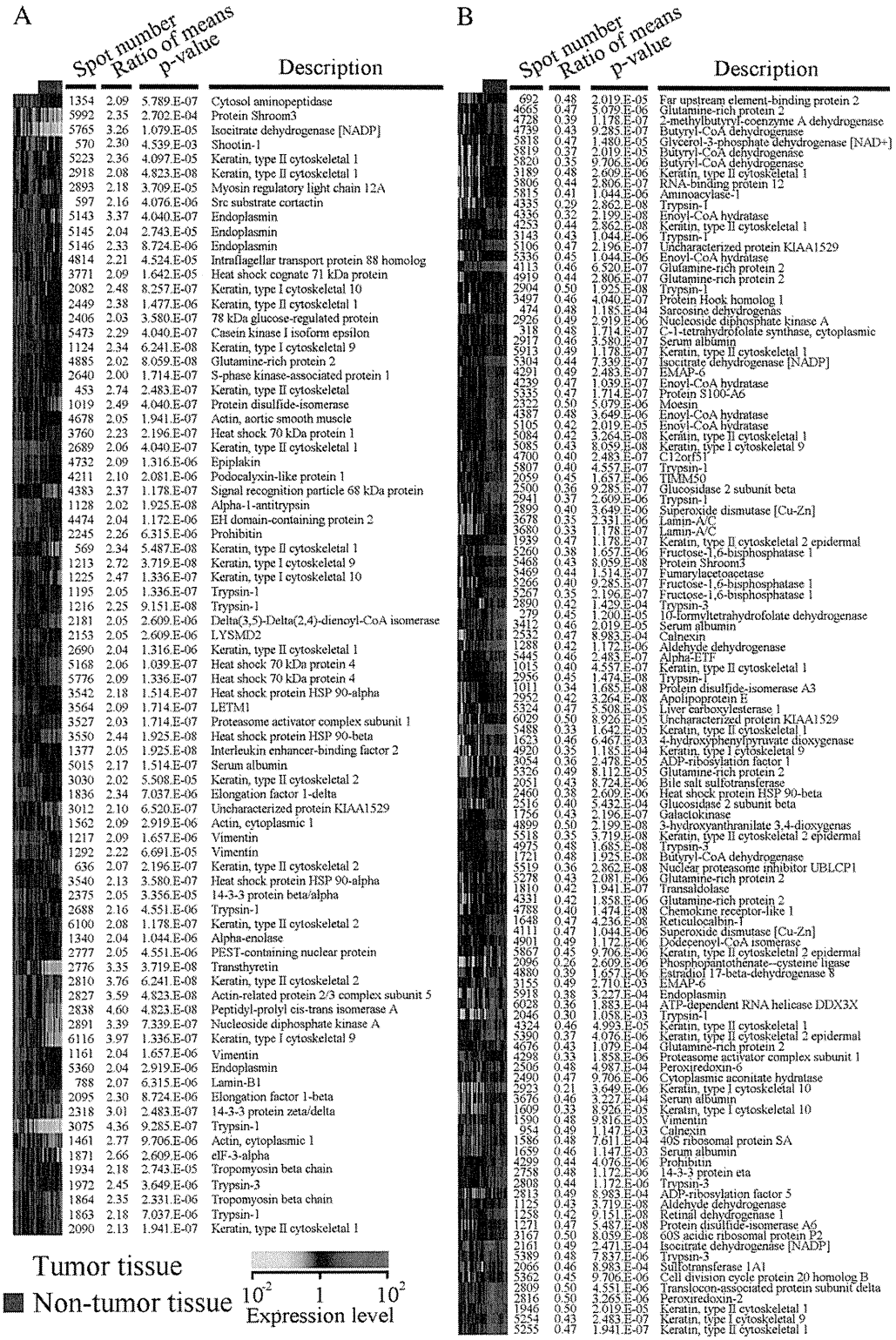

Fig. 3 – One hundred and ninety-seven protein spots with differing intensities between the tumor and non-tumor tissue groups. The ratio of means was calculated by dividing the average intensity of the tumor tissue samples with those of the non-tumor tissue samples. A: Data of 80 protein spots with higher intensities in the tumor tissue sample group are summarized. B: Data of 117 protein spots with lower intensities in the tumor tissue sample groups are summarized. The localization of these protein spots is shown in Supplementary Fig. 1, and the detailed data for protein identification is shown in Supplementary Tables 3 and 4.